
Little By Little: Continual Learning via Self-Activated Sparse Mixture-of-Rank Adaptive Learning

Haodong Lu^{1,2} Chongyang Zhao¹ Jason Xue²

Lina Yao^{2,1} Kristen Moore² Dong Gong^{1*}

¹University of New South Wales, ²CSIRO’s Data61

{haodong.lu, chongyang.zhao, dong.gong}@unsw.edu.au,

{jason.xue, lina.yao, kristen.moore}@data61.csiro.au

Abstract

Continual learning (CL) with large pre-trained models is challenged by catastrophic forgetting and task interference. Existing LoRA-based Mixture-of-Experts (MoE) approaches mitigate forgetting by assigning and freezing task-specific adapters, but suffer from interference, redundancy, and ambiguous routing due to coarse adapter-level selection. However, this design introduces three key challenges: 1) *Interference*: Activating full LoRA experts per input leads to subspace interference and prevents selective reuse of useful components across tasks. 2) *Redundancy*: Newly added experts often duplicate or contradict existing knowledge due to unnecessary activation of unrelated ranks and insufficient reuse of relevant ones. 3) *Ambiguity*: Overlapping features across tasks confuse the router, resulting in unstable expert assignments. As more experts accumulate, earlier task routing degrades, accelerating forgetting. We propose *MoRA*, a **Mixture-of-Rank Adaptive learning** approach with self-activated and sparse rank activation for CL. Unlike mixing multiple low-rank matrices, MoRA decomposes each rank- r update into r rank-1 components, each treated as an independent expert, enabling fine-grained *mixture of rank-1* expert utilization while mitigating interference and redundancy. To avoid ambiguous routing, we propose that each rank-1 expert can infer its own relevance via intermediate activations. Coupled with our proposed rank pruning and activation budgets, MoRA adaptively selects a sparse mixture of ranks per input. We validate MoRA on continual learning tasks with CLIP and large language models (LLMs), analyzing both in-domain learning and out-of-domain forgetting/generalization during fine-tuning. MoRA shows significant effectiveness on enhancing CL with PTMs, and improving generalization while mitigating forgetting.

“Little by little, we gave you everything you ever dreamed of...” — “Little by little”, Oasis.

1 Introduction

Continual learning (CL) [17, 21, 29, 43, 73] aims to enable models to incrementally and efficiently acquire new knowledge from a stream of tasks, without catastrophic forgetting [51, 55] or the need for repeated fine-tuning on all previously seen data [72, 76, 77, 85]. The emergence of large pre-trained models (PTMs), including Vision Transformer (ViT) for vision [22], Large Language Model (LLM) [28, 61], and CLIP for vision–language embeddings [33, 60], has spurred a wave exploring CL with PTMs [35, 52, 58, 59, 62, 72, 74, 81, 94]. Despite the success of PTMs, CL on them across sequential

*D. Gong is the corresponding author.

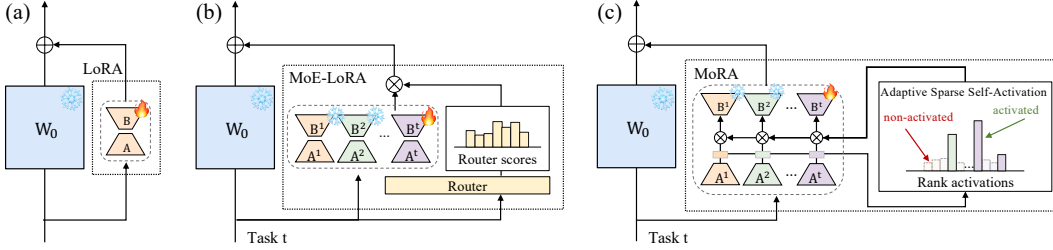


Figure 1: Conceptual illustration of CL with (a) LoRA, (b) MoE-LoRA, and (c) MoRA (Ours).

tasks still faces key challenges, including preventing catastrophic forgetting and preserving—or even enhancing—the pre-trained capabilities to generalize to unseen or future cases [48, 58, 85, 92].

A common approach to integrating new knowledge into pre-trained models (PTMs) is continual full fine-tuning [27, 92] or parameter-efficient fine-tuning (PEFT) using a small set of learnable parameters, such as Low-Rank Adaptation (LoRA) [32] (Fig. 1(a)). However, continually updating the same set of parameters often causes interference and forgetting, even with a single new task [7]. Leveraging LoRA’s inherent regularization and flexibility, many CL methods for PTMs employ LoRA or its variants, along with specialized strategies to mitigate forgetting [44, 44, 58, 72, 74, 74].

Inspired by mixture-of-experts (MoE) architectures [16, 24, 40, 65] and the modular nature of LoRA adapters, MoE frameworks using LoRA as experts (Fig. 1(b)) have been widely adopted in CL [13, 72, 84, 85]. These methods incrementally train new LoRA experts while freezing previous ones, using a router to compose experts per sample. This isolation reduces cross-task interference and forgetting, while the composability of experts supports knowledge reuse and transfer [58, 64, 72]. In MoE-LoRA models, each expert comprises a full LoRA adapter with multiple ranks (i.e., subspaces), and expert selection occurs at this coarse-grained adapter level. Despite their success, this coarse granularity and the routing mechanism introduce three key challenges that limit effective utilization:

- (1) **Interference across experts and infeasible knowledge reuse.** For any given sample, an entire LoRA expert must be either fully activated or not at all, leading to two major issues: interference among incompatible ranks from different experts, and limited flexibility in knowledge reuse.
- (2) **Learning redundancy and conflicts.** Newly added experts may relearn redundant information or learn conflicting representation due to unnecessary activation of unrelated old ranks or insufficient reuse of relevant ones. This coarse selection exacerbates interference and forgetting during inference.
- (3) **Routing ambiguity and forgetting.** Redundancy and conflicts among experts make it hard for a LoRA-level router to assign overlapping or common inputs correctly, leading to suboptimal mixtures [16, 24, 40]. As more new experts are accumulated in CL, the router’s assignments for earlier tasks become increasingly unreliable, making it more prone to forgetting.

We propose **MoRA**, a **M**ixture-of-**R**ank Adaptive learning approaches with self-activated and sparsely selected ranks across the LoRAs added at different tasks. To address the limitations of coarse-grained MoE-LoRA methods, MoRA operates at a fine-grained level by treating each *rank-one* subspace within a LoRA adapter as an individual expert. Expert selection and routing are performed at the rank level, reducing interference from activating entire LoRA blocks. This decomposition promotes specialization on narrow regions of the data manifold, reduces redundancy, and enables effective reuse of shared knowledge across tasks.

We introduce a self-activation mechanism to select a sparse set of ranks without relying on a separately trained router, avoiding routing confusion and further mitigating forgetting (Fig. 1(c)). Each rank evaluates its own relevance to the input and determines its contribution, grounded in the view of low-rank updates as linear key–value memory. Sparsity is enforced via temperature-scaled softmax together with $\text{top-}k$ masking and rank pruning under a rank activation budget. This design introduces no additional computation and eliminates the overhead associated with extra routing. Leveraging the connection between PTMs and low-dimensional manifolds [1, 41], MoRA enables precise, *input-specific adaptation* at test time through selective subspace updates. With fine-grained rank-level experts and sparse activation, MoRA facilitates continual learning by reusing relevant old ranks and selectively activating a few new ones per sample, enabling efficient, “little-by-little” adaptation that minimizes redundancy and supports essential updates. This selective, sample-specific activation at inference also enhances retention of pre-trained knowledge and improves generalization to unseen or future cases.

We apply and validate MoRA on CL with both vision-language CLIP and LLMs, as well as analyzing the effects on general pre-trained knowledge during low-rank fine-tuning. Across all settings, MoRA achieves strong downstream performance with significantly fewer active parameters, substantially reduces forgetting of both prior tasks and pre-trained knowledge, and even enhances generalization to unseen domains.

2 Related Work

Continual learning enables sequential knowledge acquisition without forgetting. Experience replay (ER) methods [4, 10, 11, 45, 49, 82, 83] interleave past examples with new data. Parameter regularization [2, 3, 34, 36, 86] penalizes updates to critical weights. Dynamic networks [44, 52, 66, 70–72, 72, 75–77, 93] allocate new capacity on the fly and preserve dedicated pathways for prior tasks.

Continual learning of PTMs. For CL on vision–language CLIP model [27, 35, 89], methods like ZSCL [92] retain zero-shot performance during adaptation, and follow-up work [48, 67, 81, 85] continually fine-tunes while leveraging frozen pre-trained predictions. The X-TAIL benchmark [81] further challenges models by mixing domain labels at test time. In large language models (LLMs) [18, 58, 59, 62, 74], continual learning uses capacity expansion or task-specific submodules to reduce interference. In this work, we also study how fine-tuning impacts pre-trained general knowledge.

Low-rank adaptation (LoRA) [32] is widely used for parameter-efficient fine-tuning of large pre-trained models. Building on this foundation, recent methods reformulate LoRA’s updates via SVD-based initialization and dynamic rank scheduling [20, 46, 53, 79, 87, 88], showing that task adaptation primarily lies in a compact subspace. In this work, we offer a complementary perspective by viewing both pre-trained weight matrix and its low-rank updates as a linear associative memory [1, 5, 37, 41]. Under this lens, a rank- r update corresponds to writing r new key–value entries into the pre-trained memory matrix, with each rank-1 component acting as an independent memory slot.

Mixture-of-experts (MoE) in LoRA fine-tuning. MoE increases model capacity by replacing the Transformer’s feed-forward layer with expert subnetworks, routing each input to a small subset and using load-balancing losses to even out usage [16, 24, 40, 65]. This paradigm has been adapted for standard fine-tuning [14, 23, 42] and CL [13, 72, 84, 85] with LoRA, treating each low-rank adapter as an expert: new adapters are trained and frozen per task to prevent forgetting. In contrast, we decompose each rank- r update into r rank-1 components and compute an input-dependent mixture over these fine-grained experts, greatly enhancing both expert specialization and mixture diversity.

3 Methods

3.1 Preliminaries

Continual learning. In continual learning, a model must sequentially learn from T distinct tasks. For task $t \in \{1, \dots, T\}$, we denote its dataset by $\mathcal{D}^t = \{(\mathbf{x}_i^t, y_i^t)\}_{i=1}^{N^t}$, where $\mathbf{x}_i^t \in \mathbb{R}^{H \times W \times C}$ is the i th input sample, $y_i^t \in \mathcal{C}^t$ is its desired prediction, and N^t is the number of examples in task t . At each time step t , the model may only access \mathcal{D}^t and is prohibited from storing or replaying data from any \mathcal{D}^u with $u < t$. This constraint makes it challenging to avoid catastrophic forgetting, which updates on new tasks overwrite knowledge acquired on earlier ones.

Low-rank adaptation. LoRA [32] parameterizes a low-rank update to a pre-trained weight matrix $\mathbf{W}_0 \in \mathbb{R}^{d_{out} \times d_{in}}$ by introducing two factors $\mathbf{B} \in \mathbb{R}^{d_{out} \times r}$ and $\mathbf{A} \in \mathbb{R}^{r \times d_{in}}$, such that $\Delta \mathbf{W} = \mathbf{B}\mathbf{A}$, where $r \ll \min(d_{in}, d_{out})$. The updated weight matrix is then defined as:

$$\mathbf{W} = \mathbf{W}_0 + \Delta \mathbf{W} = \mathbf{W}_0 + \mathbf{B}\mathbf{A}. \quad (1)$$

In this formulation, the original weights \mathbf{W}_0 remain fixed, and only \mathbf{B} and \mathbf{A} are trained, reducing the number of trainable parameters from $d_{in}d_{out}$ to $r(d_{in} + d_{out})$.

Mixture-of-Experts LoRA. Building on the Mixture-of-Experts (MoE) paradigm, a common framework of MoE-LoRA [72, 85] treats each LoRA as an independent expert and incrementally adds a new LoRA expert for each incoming task. After T tasks, we have T LoRA experts $\{(\mathbf{A}^1, \mathbf{B}^1), \dots, (\mathbf{A}^T, \mathbf{B}^T)\}$. For an input token $x \in \mathbb{R}^{d_{in}}$, the overall LoRA update in this framework is given by $\Delta \mathbf{W} = \sum_{i=1}^T R(x)_i \mathbf{B}^i \mathbf{A}^i$, where the mixture weight $R(x) \in \mathbb{R}^T$ is produced by a

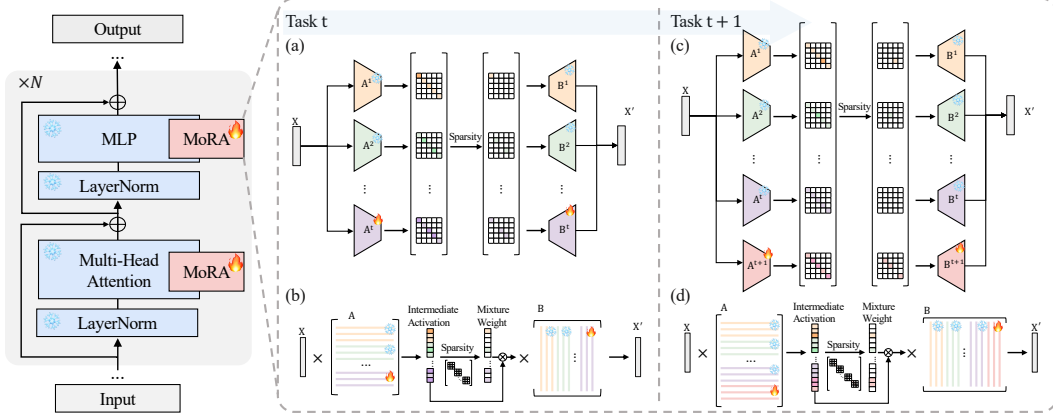


Figure 2: Overview of MoRA. For each new task, we freeze the ranks learned on previous tasks and introduce r new ranks of updates. Our sparse self-activated mixture-of-ranks framework jointly considers all old and new ranks, adaptively inferring a sparse mixture weight for each rank. Panels (a,c) illustrate MoRA conceptually and (b,d) detail its computation for tasks t and $t + 1$, respectively.

learned router $R(\cdot) = \text{softmax}(x\mathbf{W}_r)$ and $\mathbf{W}_r \in \mathbb{R}^{d_{\text{in}} \times T}$ contains the router’s trainable parameters. Each LoRA’s contribution is weighted by the learnable router, enabling the model to dynamically select and combine the most relevant low-rank updates for each token. In practice, a top- k masking is typically applied to mixture weights to enforce sparsity, activating only the k most relevant experts and controlling computational overhead.

3.2 Pre-trained Weight Matrices and Low-Rank Updates as Linear Associative Memory

Large PTMs have been shown to lie on a low “intrinsic dimension” manifold [1, 41]. From this perspective, the pre-trained weight matrix $\mathbf{W}_0 \in \mathbb{R}^{d_{\text{out}} \times d_{\text{in}}}$ can itself be viewed as a linear associative memory [5, 37], having stored key–value pair of memories drawn from vast pre-training data. Specifically, any rank- r update $\Delta\mathbf{W} = \mathbf{B}\mathbf{A}$ can be viewed as inserting or updating r key–value entries into the pre-trained weight matrix. Concretely, let

$$\mathbf{A} = [\mathbf{A}_1^\top \quad \dots \quad \mathbf{A}_r^\top]^\top \in \mathbb{R}^{r \times d_{\text{in}}}, \quad \mathbf{B} = [\mathbf{B}_1 \quad \dots \quad \mathbf{B}_r] \in \mathbb{R}^{d_{\text{out}} \times r}, \quad (2)$$

where each $\mathbf{A}_i \in \mathbb{R}^{1 \times d_{\text{in}}}$ serves as a key and each $\mathbf{B}_i \in \mathbb{R}^{d_{\text{out}} \times 1}$ as its corresponding value. Then

$$\Delta\mathbf{W} = \sum_{i=1}^r \mathbf{B}_i \mathbf{A}_i \quad (3)$$

writes the value \mathbf{B}_i into the memory slot addressed by key \mathbf{A}_i . In this associative-memory view, each rank- i component explicitly encodes “what to store” (the value \mathbf{B}_i) and “how to index it” (the key \mathbf{A}_i), thereby enriching the base model with newly acquired knowledge. More details are left in Appendix A.

3.3 Mixture of Ranks Adaptation

To overcome the *coarse granularity* of MoE-LoRA, we introduce mixture-of-ranks, applying MoE at the rank-level subspace within all LoRA adapters. By treating each rank as an independent expert, our fine-grained mixture framework enables: 1. *Reduced redundancy and shared knowledge reuse*: encoding common, cross-task features (e.g., generic semantics) can be reused, preventing redundant relearning. 2. *Minimized interference and enhanced specialization*: focusing exclusively on task-specific patterns, ensuring that new knowledge is learned without disrupting existing representations or interfered with future updates.

For any given input token x from task t , we weight each rank’s contribution according to its relevance. We introduce a scalar mixture weight $w_i \in \mathbb{R}$ for each rank, yielding

$$\Delta\mathbf{W}^t = \sum_{i=1}^{r_t} w_i \mathbf{B}_i \mathbf{A}_i, \quad (4)$$

where each rank-1 update is analogous to an independent expert, r_t is the total number of ranks learned up to task t , and w_i modulates whether and how strongly the corresponding rank contributes

to the final updated weight matrix. Unlike prior work that treats the entire rank- r update as one expert [72, 85], this formulation enables fine-grained utilization of each rank’s update.

3.4 Self-Activated Adaptive Sparse Mixture of Ranks

Another key challenge in MoE and continual learning is the *routing ambiguity and forgetting*. To this end, we explore whether each rank-1 expert can autonomously infer its relevance to the current input, eliminating the need for a separate router and enabling self-activated expert selection.

Self-activated sparse mixture of ranks. Rather than relying on an external router, our framework derives mixture weights for each rank directly from the activations of each rank. Recall from Eq. (3) that each rank- i update is parameterized by a key-value pair $(\mathbf{A}_i, \mathbf{B}_i)$. Given an input token $x \in \mathbb{R}^{d_{in}}$ from task t , by treating \mathbf{A} as the set of keys, we compute a raw score for all r_t ranks accumulated up to task t :

$$s_i = \frac{\mathbf{A}_i x}{\sqrt{\sum_{j=1}^{r_t} \|\mathbf{A}_j x\|_2^2}} \in \mathbb{R}, \tag{5}$$

where the ℓ_2 -normalization over all r_t ranks ensures numerical stability and compensates for variations in activation scales between layers and pre-trained weights. As shown in Table 5, using these raw scores alone matches or even exceeds the performance of a learned router for each rank, showing the feasibility that each rank can infer its own relevance using its activations.

To encourage rank specialization and focus the update on the most relevant ranks, we temperature-scale and normalize the scores:

$$w_i = \text{softmax}\left(\frac{s}{\tau_{\text{MoRA}}}\right)_i, \tag{6}$$

where the softmax is taken over the vector $s = [s_1, \dots, s_{r_t}]$ and τ_{MoRA} is a temperature hyperparameter that controls the sharpness of the distribution. To ensure only a sparse, specialized subset of ranks contributes, we introduce an activation budget that caps the number of ranks that can be activated.

Adaptive sparse mixture of ranks. To ensure a stable and sparse activation pattern, we impose a fixed sparse rank-activation budget via top- k masking on the ℓ_2 -normalized scores $s_i := \text{TopK}(s, k)$, where

$$[\text{TopK}(s, k)]_i = \begin{cases} s_i, & \text{if } s_i \text{ is among the top } k \text{ entries of } s, \\ -\infty, & \text{otherwise,} \end{cases} \tag{7}$$

ensuring a sparse subset of at most k out of the total r_t ranks to be activated for task t during CL.

We further refine the mixture weights by applying a fixed threshold δ to the ℓ_2 -normalized scores s_i . Concretely, after computing the softmax weights w_i , we define a binary mask $m_i = \mathbb{1}\{s_i \geq \delta\}$, and update each gate via $w_i := m_i \odot w_i$, where $\mathbb{1}\{\cdot\}$ is an indicator function and \odot denotes element-wise multiplication. This mask zeroes out any rank whose normalized activation falls below the threshold, ensuring that only the most relevant ranks contribute, resulting in a sparse mixture of an adaptive number of ranks based on the input.

Incremental mixture of ranks. Unlike methods that add a fixed number of LoRA experts per task [85], MoRA incrementally adds r new ranks for each task, freezes all prior ranks, and adaptively selects a sparse subset of the most relevant ranks during both training and inference. This design seamlessly incorporates new task-specific knowledge into freshly initialized ranks while preserving earlier ranks unchanged to prevent forgetting. Moreover, it facilitates common knowledge reuse by allowing ranks that encode common patterns to be activated in later tasks.

Training Objectives. In our experiments, we only use the model’s standard training objective, without any extra regularization or load-balancing constraints. In practice, we empirically observe that the conventional load-balancing loss widely employed in the Mixture-of-Experts literature [16, 24, 40, 65] is not necessary, thanks to our fine-grained self-activated gating design. Imposing a strict load-balancing constraint might hinder the learning of the key vectors (*i.e.*, matrix \mathbf{A}), since each rank should remain free to capture its own characteristic input distribution. Fig. 3 illustrates how each rank learns distinct characteristics.

Table 1: Comparisons on X-TAIL for each domain in terms of “Transfer”, “Average”, and “Last” scores (%). The **best** and the **second best** results are highlighted in **red** and **blue**, respectively.

Method	Aircraft [50]	Caltech101 [25]	DTD [15]	EuroSAT [30]	Flowers [56]	Food [8]	MINIST [19]	OxfordPet [57]	Cars [38]	SUN397 [80]	Average
<i>CLIP</i>											
Zero-shot	23.5	76.8	37.3	36.7	63.6	84.0	46.7	86.7	66.1	63.7	58.5
<i>Transfer</i>											
Zero-shot [60]	–	76.8	37.3	36.7	63.6	84.0	46.7	86.7	66.1	63.7	62.4
LwF [43]	–	66.6	26.9	19.5	51.0	78.4	26.6	68.9	35.5	56.1	47.7
WiSE-FT [78]	–	70.1	31.9	25.3	56.3	79.8	29.9	74.9	45.6	56.8	52.3
iCaRL [63]	–	71.7	35.0	43.0	63.4	86.9	43.9	87.8	63.7	60.0	61.7
ZSCL [92]	–	73.3	32.6	36.8	62.1	83.8	42.1	83.6	56.5	60.2	59.0
MoE-Adapter [85]	–	71.0	34.9	19.2	63.0	86.6	20.0	87.2	63.7	58.6	56.0
RAIL-Primal [81]	–	76.8	37.3	36.7	63.6	84.0	46.7	86.7	66.1	63.7	62.4
CoDyRA [48]	–	74.3	36.8	44.2	69.9	83.5	42.8	88.9	64.6	63.4	63.2
MoRA	–	74.5	38.1	46.9	65.3	82.9	45.8	88.2	65.1	62.9	63.3
<i>Average</i>											
LwF [43]	24.7	79.7	38.3	36.9	63.9	81.0	36.5	71.9	42.7	56.7	53.2
WiSE-FT [78]	27.1	76.5	40.9	31.3	68.7	81.6	31.4	74.7	51.7	58.4	54.2
iCaRL [63]	25.4	72.1	37.5	51.6	65.1	87.1	59.1	88.0	63.7	60.1	61.0
ZSCL [92]	36.0	75.0	40.7	40.5	71.0	85.3	46.3	83.3	60.7	61.5	60.0
MoE-Adapter [85]	43.6	77.9	52.1	34.7	75.9	86.3	45.2	87.4	66.6	60.2	63.0
RAIL-Primal [81]	42.4	89.8	55.7	68.5	84.0	83.3	65.3	85.8	67.9	64.5	70.7
CoDyRA [48]	41.4	81.0	58.7	77.8	83.4	84.6	64.5	90.4	67.2	64.4	71.3
MoRA	44.1	81.6	64.6	79.6	83.9	84.4	66.5	89.7	68.4	64.1	72.7
<i>Last</i>											
LwF [43]	25.5	72.1	38.9	55.4	65.5	87.3	81.9	88.6	63.6	61.5	64.0
WiSE-FT [78]	21.8	76.8	42.9	20.8	77.5	84.9	30.7	76.6	75.8	72.5	58.0
iCaRL [63]	25.5	72.1	38.9	55.4	65.5	87.3	81.9	88.6	63.6	61.5	64.0
ZSCL [92]	33.1	75.3	43.5	35.2	74.6	87.4	50.4	84.2	77.3	73.4	63.4
MoE-Adapter [85]	43.2	78.7	57.6	32.8	79.4	86.0	86.7	87.8	78.2	74.2	70.5
RAIL-Primal [81]	41.7	94.0	66.0	86.4	97.2	82.4	93.1	83.6	75.0	71.3	79.1
CoDyRA [48]	37.7	81.5	65.1	89.9	91.4	85.5	96.8	93.3	77.3	73.5	79.2
MoRA	37.7	81.5	70.7	92.4	95.0	86.0	97.6	92.6	81.0	74.7	80.9

4 Experiments

In this paper, we conduct experiments across a diverse set of tasks, including continual learning for both vision-language CLIP models and LLMs, and analyze catastrophic forgetting during fine-tuning. Detailed implementation settings and more experiment results are provided in the Appendix.

CL of CLIP We evaluate on two benchmarks using CLIP-ViT/B-16 [33, 60]: MTIL [85, 92], with 11 datasets learned sequentially under a 5-shot split, and X-TAIL [48, 81], with a 16-shot split. Following prior work, we report Transfer (zero-shot on unseen tasks), Last (retention on earlier tasks), and Average (mean of Transfer and Last) to assess continual learning performance.

CL of LLM. We follow prior work [58, 59, 62, 74] to continually fine-tune T5-large [61] on five text-classification benchmarks—AG News, Amazon Reviews, Yelp Reviews, DBpedia, and Yahoo Answers—under three different task orderings. We report the average final accuracy across all tasks after completing the last task, measuring the model’s ability to retain knowledge during CL.

Generalization and forgetting on unseen tasks. To assess effects on pre-trained general knowledge, we fine-tune Llama3 [28] on the CodeAlpaca code-generation dataset [9] and evaluate zero-shot in-domain performance on HumanEval [12], as well as out-of-domain accuracy on a broad selection of MMLU [31] subjects—Formal Logic, Philosophy, World Religions, Economics, Public Relations, STEM, Physics, and Machine Learning. These results reveal how fine-tuning impacts both task-specific adaptation and catastrophic forgetting or improved generalization to unseen domains.

4.1 Continual Learning of CLIP

Cross-domain task-agnostic incremental learning. Table 1 presents our results on the X-TAIL benchmark. Prior methods [81, 85] rely on zero-shot predictions to preserve pre-trained capabilities and mitigate forgetting, and as a result are capped by the base model’s zero-shot performance.

Table 2: Comparisons on 5-shot MTIL setting. Following the same protocol as in [48, 81, 85].

Method	Aircraft [50]	Caltech101 [25]	CIFAR100 [39]	DTD [15]	EuroSAT [30]	Flowers [56]	Food [8]	MNIST [19]	OxfordPet [57]	Cars [38]	SUN397 [80]	Average
<i>CLIP</i>												
Zero-shot [60]	24.3	88.4	68.2	44.6	54.9	71.0	88.5	59.4	89.0	64.7	65.2	65.3
<i>Transfer</i>												
Zero-shot [60]	-	88.4	68.2	44.6	54.9	71.0	88.5	59.6	89.0	64.7	65.2	69.4
LwF [43]	-	72.1	49.2	35.9	44.5	41.1	66.6	50.5	69.0	19.0	51.7	50.0
LwF-VR [21]	-	82.2	62.5	40.1	40.1	56.3	80.0	60.9	77.6	40.5	60.8	60.1
WiSE-FT [78]	-	77.6	60.0	41.3	39.4	53.0	76.6	58.1	75.5	37.3	58.2	57.7
ZSCL [92]	-	84.0	68.1	44.8	46.8	63.6	84.9	61.4	81.4	55.5	62.2	65.3
MoE-Adapter [85]	-	87.9	68.2	44.1	48.1	64.7	88.8	69.0	89.1	64.5	65.1	68.9
RAIL-Primal [81]	-	88.4	68.2	44.6	54.9	71.0	88.5	59.6	89.0	64.7	65.2	69.4
CoDyRA [48]	-	92.4	68.4	45.8	54.5	69.6	87.4	65.2	88.5	64.2	64.5	69.9
MoRA	-	92.0	68.8	45.6	53.1	68.6	84.4	64.3	89.8	65.4	64.8	69.7
<i>Average</i>												
LwF [43]	23.5	77.4	43.5	41.7	43.5	52.2	54.6	63.4	68.0	21.3	52.6	49.2
LwF-VR [21]	24.9	89.1	64.2	53.4	54.3	70.8	79.2	66.5	79.2	44.1	61.6	62.5
WiSE-FT [78]	32.0	87.7	61.0	55.8	68.1	69.3	76.8	71.5	77.6	42.0	59.3	63.7
ZSCL [92]	28.2	88.6	66.5	53.5	56.3	73.4	83.1	56.4	82.4	57.5	62.9	64.4
MoE-Adapter [85]	30.0	89.6	73.9	58.7	69.3	79.3	88.1	76.5	89.1	65.3	65.8	71.4
RAIL-Primal [81]	32.9	94.5	69.9	58.1	71.8	84.4	88.5	70.4	89.0	66.1	65.7	71.9
CoDyRA [48]	34.6	95.8	73.9	60.0	77.1	81.3	86.6	75.9	89.9	66.1	65.3	73.3
MoRA	36.7	95.4	74.9	61.9	77.1	82.6	85.3	76.0	90.5	67.0	65.6	73.9
<i>Last</i>												
LwF [43]	22.1	58.2	17.9	32.1	28.1	66.7	46.0	84.3	64.1	31.5	60.1	46.5
LwF-VR [21]	22.9	89.8	59.3	57.1	57.6	79.2	78.3	77.7	83.6	60.1	69.8	66.9
WiSE-FT [78]	30.8	88.9	59.6	60.3	80.9	81.7	77.1	94.9	83.2	62.8	70.0	71.9
ZSCL [92]	26.8	88.5	63.7	55.7	60.2	82.1	82.6	58.6	85.9	66.7	70.4	67.4
MoE-Adapter [85]	30.1	89.3	74.9	64.0	82.3	89.4	87.1	89.0	89.1	69.5	72.5	76.1
RAIL-Primal [81]	32.9	95.1	70.3	63.2	81.5	95.6	88.5	89.7	89.0	72.5	71.0	77.2
CoDyRA [48]	31.6	95.5	72.8	63.5	85.0	89.7	85.0	94.7	93.2	73.6	73.0	78.0
MoRA	32.5	95.3	75.3	66.6	87.8	92.6	86.3	96.3	92.6	73.5	73.8	79.3

Similarly as done in previous works [48, 92], MoRA aims to continuously refine the pre-trained model, enabling it to surpass this zero-shot ceiling and improve the generalization of the pre-trained model on unseen domains. In practice, continual parameter updates can slightly perturb some zero-shot predictions, our method ultimately improves overall performance on unseen domains by adapting the pre-trained model to new tasks while enhancing its generalization capabilities.

On the Last and Average metrics, MoRA significantly outperforms prior methods. Unlike approaches that require domain ID prediction [85], high dimensional projection layers, or a memory bank of feature embeddings [81], MoRA enhances the pre-trained model’s own representation capability without relying on these external mechanisms. In contrast to the previous state of the art [48], which learns a fixed weight for each rank- r update from each task, MoRA’s novel mixture-of-ranks framework selectively assigns each rank an input-dependent gate. Notably, only a small subset of ranks most relevant to each token are activated, resulting in far more fine-grained utilization and specialization of each ranks.

Multi-domain task incremental learning. We evaluate MoRA in the few-shot MTIL setting (Table 2) under the same protocols as [48, 81, 85]. Consistent with the results observed in the X-TAIL setting, our method demonstrates clear superiority in this scenario.

4.2 Continual Learning of LLM

Table 3 reports results across three task orderings, where MoRA consistently outperforms prior methods and nearly matches the multi-task learning (MTL) upper bound. In contrast to state-of-the-art

Table 3: Summary of the results on standard CL benchmarks with T5-large model. The averaged accuracy after training on the last task is reported. Experiments on long task sequences in Table 9.

Method	Standard CL Benchmark			
	Order-1	Order-2	Order-3	Avg.
MTL	80.0			
SeqFT	18.9	24.9	41.7	28.5
SeqLoRA	44.6	32.7	53.7	43.7
IncLoRA	66.0	64.9	68.3	66.4
Replay	55.2	56.9	61.3	57.8
EWC	48.7	47.7	54.5	50.3
LwF	54.4	53.1	49.6	52.3
L2P	60.3	61.7	61.1	60.7
LFPT5	67.6	72.6	77.9	72.7
O-LoRA	75.4	75.7	76.3	75.8
LB-CL	76.9	76.5	76.8	76.7
MoRA	77.43	77.47	77.93	77.61

Table 4: Fine-tuning Llama3.1-8B on the code generation domain (CodeAlpaca). We report zero-shot in-domain performance on HumanEval (Pass@1) and zero-shot out-of-domain accuracy for selected MMLU subjects—Formal Logic, Philosophy, World Religions, Economics, Public Relations, STEM, Physics, and Machine Learning. The last two columns list trainable parameters (for MoRA: added / activated). The **best** and **second best** scores are highlighted in **red** and **blue**, respectively.

Method	HumanEval (Pass@1)	Out-of-Domain (Acc.)									Params (M)	%Params
		Logic	Phil.	Reli.	Econ.	Pub. Rel.	STEM	Phys.	ML	MMLU		
Llama-3.1-8B	38.40	42.06	71.06	83.63	70.17	68.18	54.84	39.22	40.18	63.45	—	—
LoRA ($r = 4$)	41.46	39.68	70.09	81.87	71.43	65.45	54.77	45.10	40.17	63.28	10.5	0.13%
LoRA ($r = 8$)	44.51	39.68	70.74	81.87	71.85	64.54	54.17	42.16	39.29	63.03	21.0	0.26%
LoRA ($r = 16$)	45.73	41.27	68.49	80.70	72.69	66.36	54.96	44.11	38.39	63.35	41.9	0.52%
LoRA ($r = 32$)	47.56	42.85	69.45	81.87	72.27	66.36	55.44	45.10	39.29	63.59	83.9	1.03%
MoRA	47.56	48.41	70.09	82.46	73.53	68.18	55.53	46.08	41.96	63.70	41.9/26.2	0.52%/0.32%

techniques such as O-LoRA [74] and LB-CL [58], which rely on orthogonality constraints or gradient projections between per-task LoRA adapters—potentially limiting each adapter’s capacity—MoRA requires no additional regularization. By decomposing each rank- r update into its rank-1 components and applying self-activated, sparse gating, MoRA allows every component to specialize on its own input distribution. This fine-grained specialization both prevents interference across tasks and more effectively captures diverse patterns.

4.3 Forgetting and Generalization during Fine-Tuning

Table 4 examines how standard fine-tuning affects both in-domain performance and out-of-domain generalization. We observe two key phenomena: 1. *Forgetting of unrelated knowledge*. Fine-tuning with a conventional LoRA leads to performance drops on topics completely unrelated to the fine-tuning data—for example, Philosophy, World Religions, and Public Relations—indicating that the model loses pre-trained general knowledge when adapting to a new domain. 2. *Improved generalization*. Fine-tuning on code generation data also boosts accuracy on tasks requiring logical understanding (Formal Logic, Economics, STEM, Physics, and Machine Learning), suggesting that representations learned during code fine-tuning transfer to related symbolic and quantitative domains.

By contrast, MoRA’s self-routed, sparse mixture-of-ranks framework both preserves unrelated general knowledge and enhances in-domain and out-of-domain generalization performance. By decomposing each low-rank update into specialized rank-1 components and activating only the most relevant subset, MoRA prevents catastrophic overwriting of prior knowledge. At the same time, it achieves strong code-generation performance using only one-third of the activated parameters required by a rank-32 LoRA, and significantly improves the out-of-domain generalization.

4.4 Visualizations on Fine-grained Rank Activations

We visualize rank activations during continual learning in Fig. 3. These visualizations demonstrate that MoRA (1) encourages each rank to specialize in its own input distribution, and (2) reduces cross-task interference to mitigate forgetting.

Each rank specializes in distinct input patterns. In Fig. 6a, we observed that patches corresponding to the airplane object strongly activate rank 0, whereas background patches (blue sky) predominantly activate rank 11. Similarly as in Fig. 6c, ranks at index 19, 20, and 29 (highlighted with orange bounding boxes) are activated for image patches of jaguar. Moreover, the complex background elements in Fig. 6c—such as tree leaves and shadows—elicit a more diverse activation pattern than the simple blue-sky backgrounds in Fig. 6a, illustrating MoRA’s capacity to capture varying contextual complexity. Interestingly, we also observe that certain ranks learned on earlier tasks remain active when processing later-task inputs, indicating effective knowledge reuse.

Reduced cross-task interference to mitigate forgetting. By comparing the activation patterns in Fig. 6a (after learning Task 1) and Fig. 6b (after learning Task 2) on the same input image, we observe that the ranks activations are nearly identical: rank 0 continues to respond to airplane semantics, and rank 11 continues to respond to background blue-sky patches. This consistency demonstrates that our self-activated sparse mixture-of-ranks framework effectively prevents later-task updates from overwriting or intruding upon the knowledge learned for earlier tasks. As a result, inter-task interference is greatly reduced, and catastrophic forgetting is mitigated.

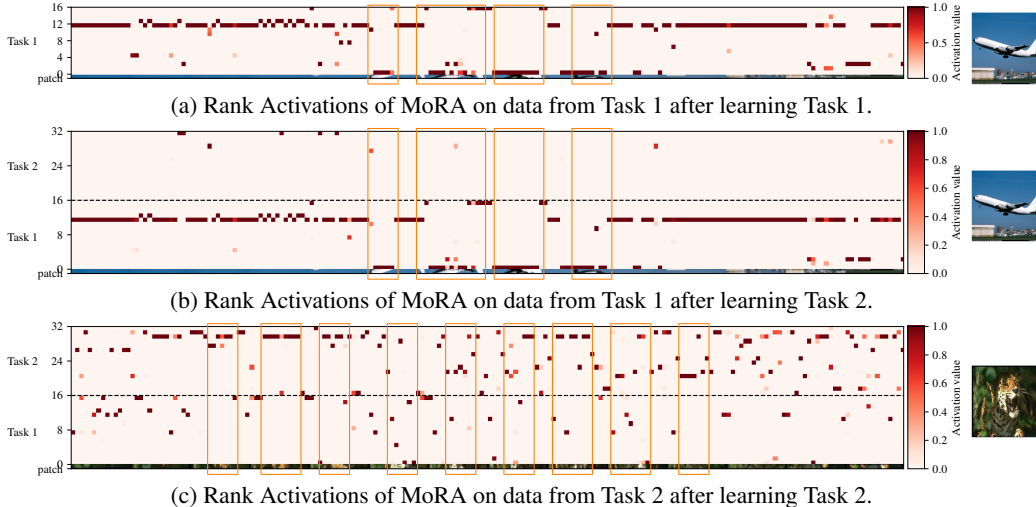


Figure 3: Visualization of MoRA rank activations during Task 1 and Task 2 training. Activations are extracted from the K projection in the attention module (layer 8) of the image encoder. Corresponding image patches are shown below each activation map, with regions relevant to each class marked by orange bounding boxes. Zoom in for details. More visualizations are in Figs. 5 and 6 of Appendix.

Table 5: Comparisons on different per LoRA/rank mixture calculation strategy

Mixture Calculation	Transfer	Average	Last
Router@LoRA	62.56	69.45	74.53
Router@rank	60.09	65.97	69.76
Self-activated@rank	60.26	65.94	69.85
+ Sparse activation	62.59	72.28	80.22
+ Adaptive sparse (MoRA)	63.30	72.70	80.90

4.5 Ablation Studies

Per-LoRA/rank mixture weights. Table 5 compares different strategies for computing mixture weights, under a controlled setup with one LoRA per task, standard training loss only, and no additional regularization: (1) *Router@LoRA* trains a standard router to assign weights to each LoRA adapter. (2) *Router@rank* trains a fine-grained router for every rank-1 component, which increases training complexity and underperforms Router@LoRA. (3) *Self-activated@rank* directly infer mixture weights using softmax-normalized activations (Eq. 5), matching or exceeding Router@rank and showing that each rank can infer its own relevance without extra parameters. (4) *Sparse activation* adds temperature scaling (Eq. 6) and caps the number of activated ranks, yielding substantial gains by sharpening rank specialization. (5) *Adaptive sparse activation* further prunes low-activation ranks at test time, selecting the most relevant number of ranks to be activated adaptively for each input token, reducing noise from less relevant ranks and achieving the best overall performance.

Rank activation budget. Under our sparse rank-activation framework, we explore how many ranks are necessary by varying the activation budget (Fig. 4a). To focus exclusively on this budget parameter, we disable other sparsity enhancements, *e.g.* rank pruning. After training on 10 tasks (160 ranks total), raising the budget from 2 (1.25%) to 16 active ranks (10%) yields a dramatic boost in final accuracy, and gradually plateaus. This demonstrates that each rank specializes in a distinct input distribution, and a small, sparse subset of ranks suffices to handle diverse input distributions. Moreover, even when the budget is set very high, our self-activating gating remains robust: it still activates only the most relevant ranks for each token while suppressing contributions from less relevant ones.

Temperature setting of τ_{MoRA} . We use temperature scaling (Eq. (6)) to control mixture sharpness: lower τ_{MoRA} yields sharper activations, while higher τ_{MoRA} flattens the distribution and engages more ranks. Figure 4b shows that increasing τ_{MoRA} improves transfer to unseen tasks, even surpassing the

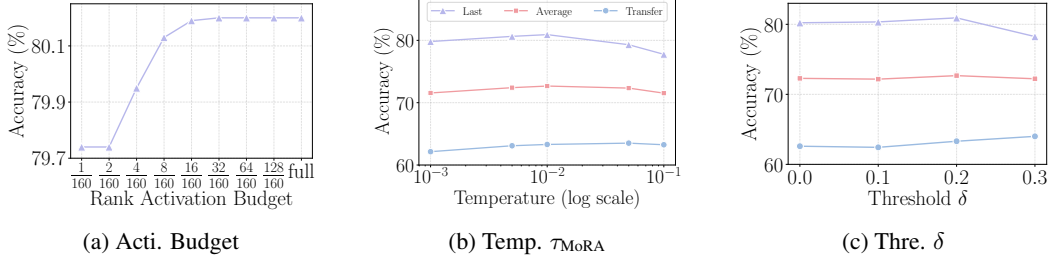


Figure 4: Ablation on (a) rank activation budget, (b) temperature τ_{MoRA} , and (c) threshold δ .

reported state-of-the-art Transfer in Table 1 when τ_{MoRA} is high. A moderate τ_{MoRA} around 0.01 balances specificity and generalization, delivering strong Last and Average scores.

Adaptive mixture with rank pruning. In Fig. 4c, we demonstrate the effects of adaptive sparsity constraints by varying the threshold δ for rank pruning. Pruning ranks with a relatively small threshold reduces noise and sharpens the mixture, improving both downstream adaptation and out-of-domain generalization, whereas raising δ above 0.2 begins to remove useful ranks and degrades performance.

5 Conclusion

We present MoRA, a self-activated sparse mixture-of-ranks framework that decomposes each LoRA update into rank-1 experts and self-infer their sparse mixture weights. By reducing knowledge redundancy and resolving router-expert mismatch during CL, MoRA delivers superior continual-learning performance, significantly reduces forgetting, and enhances generalization.

Limitations and future works. MoRA use a pre-defined temperature to control the sharpness of the mixture weights. While effective, the sparse activation mechanism can be further improved by incorporating awareness of the global data distribution. Learning this temperature or adapting the mixture’s sharpness based on data offers a promising avenue for future research. We also aim to extend the method’s applicability to a broader range of PTMs and applications.

Acknowledgments and Disclosure of Funding

This work was partially supported by the ARC DECRA Fellowship (DE230101591) awarded to D. Gong. H. Lu is affiliated with CSIRO Data61 through a PhD scholarship and acknowledges the support of the Google PhD Fellowship.

References

- [1] A. Aghajanyan, L. Zettlemoyer, and S. Gupta. Intrinsic dimensionality explains the effectiveness of language model fine-tuning. *arXiv preprint arXiv:2012.13255*, 2020.
- [2] R. Aljundi, F. Babiloni, M. Elhoseiny, M. Rohrbach, and T. Tuytelaars. Memory aware synapses: Learning what (not) to forget. In *Proceedings of the European conference on computer vision (ECCV)*, pages 139–154, 2018.
- [3] R. Aljundi, K. Kelchtermans, and T. Tuytelaars. Task-free continual learning. In *Proceedings of the IEEE/CVF Conference on Computer Vision and Pattern Recognition*, pages 11254–11263, 2019.
- [4] R. Aljundi, M. Lin, B. Goujaud, and Y. Bengio. Gradient based sample selection for online continual learning. *Advances in neural information processing systems*, 32, 2019.
- [5] J. A. Anderson. A simple neural network generating an interactive memory. *Mathematical biosciences*, 14(3-4):197–220, 1972.
- [6] D. Bau, S. Liu, T. Wang, J.-Y. Zhu, and A. Torralba. Rewriting a deep generative model. In *Computer Vision–ECCV 2020: 16th European Conference, Glasgow, UK, August 23–28, 2020, Proceedings, Part I 16*, pages 351–369. Springer, 2020.

- [7] D. Biderman, J. Portes, J. J. G. Ortiz, M. Paul, P. Greengard, C. Jennings, D. King, S. Havens, V. Chiley, J. Frankle, et al. Lora learns less and forgets less. *arXiv preprint arXiv:2405.09673*, 2024.
- [8] L. Bossard, M. Guillaumin, and L. Van Gool. Food-101—mining discriminative components with random forests. In *Proceedings of the European conference on computer vision (ECCV)*, pages 446–461, 2014.
- [9] S. Chaudhary. Code alpaca: An instruction-following llama model for code generation. <https://github.com/sahil280114/codealpaca>, 2023.
- [10] A. Chaudhry, P. K. Dokania, T. Ajanthan, and P. H. Torr. Riemannian walk for incremental learning: Understanding forgetting and intransigence. In *Proceedings of the European conference on computer vision (ECCV)*, pages 532–547, 2018.
- [11] A. Chaudhry, M. Ranzato, M. Rohrbach, and M. Elhoseiny. Efficient lifelong learning with a-gem. *arXiv preprint arXiv:1812.00420*, 2018.
- [12] M. Chen, J. Tworek, H. Jun, Q. Yuan, H. P. D. O. Pinto, J. Kaplan, H. Edwards, Y. Burda, N. Joseph, G. Brockman, et al. Evaluating large language models trained on code. *arXiv preprint arXiv:2107.03374*, 2021.
- [13] S. Chen, Z. Jie, and L. Ma. Llava-mole: Sparse mixture of lora experts for mitigating data conflicts in instruction finetuning mllms. *arXiv preprint arXiv:2401.16160*, 2024.
- [14] Z. Chen, Z. Wang, Z. Wang, H. Liu, Z. Yin, S. Liu, L. Sheng, W. Ouyang, Y. Qiao, and J. Shao. Octavius: Mitigating task interference in mllms via lora-moe. *arXiv preprint arXiv:2311.02684*, 2023.
- [15] M. Cimpoi, S. Maji, I. Kokkinos, S. Mohamed, and A. Vedaldi. Describing textures in the wild. In *Proceedings of the IEEE conference on computer vision and pattern recognition*, pages 3606–3613, 2014.
- [16] D. Dai, C. Deng, C. Zhao, R. Xu, H. Gao, D. Chen, J. Li, W. Zeng, X. Yu, Y. Wu, et al. Deepseekmoe: Towards ultimate expert specialization in mixture-of-experts language models. *arXiv preprint arXiv:2401.06066*, 2024.
- [17] M. De Lange, R. Aljundi, M. Masana, S. Parisot, X. Jia, A. Leonardis, G. Slabaugh, and T. Tuytelaars. A continual learning survey: Defying forgetting in classification tasks. *IEEE transactions on pattern analysis and machine intelligence*, 44(7):3366–3385, 2021.
- [18] C. de Masson D’Autume, S. Ruder, L. Kong, and D. Yogatama. Episodic memory in lifelong language learning. *Advances in Neural Information Processing Systems*, 32, 2019.
- [19] L. Deng. The mnist database of handwritten digit images for machine learning research [best of the web]. *IEEE signal processing magazine*, 29(6):141–142, 2012.
- [20] N. Ding, X. Lv, Q. Wang, Y. Chen, B. Zhou, Z. Liu, and M. Sun. Sparse low-rank adaptation of pre-trained language models. *arXiv preprint arXiv:2311.11696*, 2023.
- [21] Y. Ding, L. Liu, C. Tian, J. Yang, and H. Ding. Don’t stop learning: Towards continual learning for the clip model. *arXiv preprint arXiv:2207.09248*, 2022.
- [22] A. Dosovitskiy, L. Beyer, A. Kolesnikov, D. Weissenborn, X. Zhai, T. Unterthiner, M. Dehghani, M. Minderer, G. Heigold, S. Gelly, et al. An image is worth 16x16 words: Transformers for image recognition at scale. *arXiv preprint arXiv:2010.11929*, 2020.
- [23] S. Dou, E. Zhou, Y. Liu, S. Gao, J. Zhao, W. Shen, Y. Zhou, Z. Xi, X. Wang, X. Fan, et al. Loramoe: Alleviate world knowledge forgetting in large language models via moe-style plugin. *arXiv preprint arXiv:2312.09979*, 2023.
- [24] W. Fedus, B. Zoph, and N. Shazeer. Switch transformers: Scaling to trillion parameter models with simple and efficient sparsity. *Journal of Machine Learning Research*, 23(120):1–39, 2022.

- [25] L. Fei-Fei, R. Fergus, and P. Perona. Learning generative visual models from few training examples: An incremental bayesian approach tested on 101 object categories. In *2004 conference on computer vision and pattern recognition workshop*, pages 178–178. IEEE, 2004.
- [26] L. Gao, J. Tow, B. Abbasi, S. Biderman, S. Black, A. DiPofi, C. Foster, L. Golding, J. Hsu, A. Le Noac’h, H. Li, K. McDonell, N. Muennighoff, C. Ociepa, J. Phang, L. Reynolds, H. Schoelkopf, A. Skowron, L. Sutawika, E. Tang, A. Thite, B. Wang, K. Wang, and A. Zou. The language model evaluation harness, 07 2024. URL <https://zenodo.org/records/12608602>.
- [27] S. Garg, M. Farajtabar, H. Pouransari, R. Vemulapalli, S. Mehta, O. Tuzel, V. Shankar, and F. Faghri. Tic-clip: Continual training of clip models. *arXiv preprint arXiv:2310.16226*, 2023.
- [28] A. Grattafiori, A. Dubey, A. Jauhri, A. Pandey, A. Kadian, A. Al-Dahle, A. Letman, A. Mathur, A. Schelten, A. Vaughan, et al. The llama 3 herd of models. *arXiv e-prints*, pages arXiv–2407, 2024.
- [29] R. Hadsell, D. Rao, A. A. Rusu, and R. Pascanu. Embracing change: Continual learning in deep neural networks. *Trends in cognitive sciences*, 24(12):1028–1040, 2020.
- [30] P. Helber, B. Bischke, A. Dengel, and D. Borth. Eurosat: A novel dataset and deep learning benchmark for land use and land cover classification. *IEEE Journal of Selected Topics in Applied Earth Observations and Remote Sensing*, 12(7):2217–2226, 2019.
- [31] D. Hendrycks, C. Burns, S. Basart, A. Zou, M. Mazeika, D. Song, and J. Steinhardt. Measuring massive multitask language understanding. *Proceedings of the International Conference on Learning Representations (ICLR)*, 2021.
- [32] E. J. Hu, Y. Shen, P. Wallis, Z. Allen-Zhu, Y. Li, S. Wang, L. Wang, and W. Chen. Lora: Low-rank adaptation of large language models. *arXiv preprint arXiv:2106.09685*, 2021.
- [33] G. Ilharco, M. Wortsman, R. Wightman, C. Gordon, N. Carlini, R. Taori, A. Dave, V. Shankar, H. Namkoong, J. Miller, H. Hajishirzi, A. Farhadi, and L. Schmidt. Openclip, July 2021. URL <https://doi.org/10.5281/zenodo.5143773>.
- [34] S. Jha, D. Gong, H. Zhao, and L. Yao. Npcl: Neural processes for uncertainty-aware continual learning. *arXiv preprint arXiv:2310.19272*, 2023.
- [35] S. Jha, D. Gong, and L. Yao. CLAP4CLIP: Continual learning with probabilistic finetuning for vision-language models. In *The Thirty-eighth Annual Conference on Neural Information Processing Systems*, 2024. URL <https://openreview.net/forum?id=rF1YRtZfoJ>.
- [36] J. Kirkpatrick, R. Pascanu, N. Rabinowitz, J. Veness, G. Desjardins, A. A. Rusu, K. Milan, J. Quan, T. Ramalho, A. Grabska-Barwinska, et al. Overcoming catastrophic forgetting in neural networks. *Proceedings of the national academy of sciences*, 114(13):3521–3526, 2017.
- [37] T. Kohonen. Correlation matrix memories. *IEEE transactions on computers*, 100(4):353–359, 1972.
- [38] J. Krause, M. Stark, J. Deng, and L. Fei-Fei. 3d object representations for fine-grained categorization. In *Proceedings of the IEEE international conference on computer vision workshops*, pages 554–561, 2013.
- [39] A. Krizhevsky, G. Hinton, et al. Learning multiple layers of features from tiny images. 2009.
- [40] D. Lepikhin, H. Lee, Y. Xu, D. Chen, O. Firat, Y. Huang, M. Krikun, N. Shazeer, and Z. Chen. Gshard: Scaling giant models with conditional computation and automatic sharding. *arXiv preprint arXiv:2006.16668*, 2020.
- [41] C. Li, H. Farkhoor, R. Liu, and J. Yosinski. Measuring the intrinsic dimension of objective landscapes. *arXiv preprint arXiv:1804.08838*, 2018.
- [42] D. Li, Y. Ma, N. Wang, Z. Ye, Z. Cheng, Y. Tang, Y. Zhang, L. Duan, J. Zuo, C. Yang, et al. Mixlora: Enhancing large language models fine-tuning with lora-based mixture of experts. *arXiv preprint arXiv:2404.15159*, 2024.

- [43] Z. Li and D. Hoiem. Learning without forgetting. *IEEE transactions on pattern analysis and machine intelligence*, 40(12):2935–2947, 2017.
- [44] Y.-S. Liang and W.-J. Li. Infloa: Interference-free low-rank adaptation for continual learning. In *Proceedings of the IEEE/CVF Conference on Computer Vision and Pattern Recognition*, pages 23638–23647, 2024.
- [45] Y. Liu, Y. Su, A.-A. Liu, B. Schiele, and Q. Sun. Mnemonics training: Multi-class incremental learning without forgetting. In *Proceedings of the IEEE/CVF conference on Computer Vision and Pattern Recognition*, pages 12245–12254, 2020.
- [46] Z. Liu, J. Lyn, W. Zhu, X. Tian, and Y. Graham. Alora: Allocating low-rank adaptation for fine-tuning large language models. *arXiv preprint arXiv:2403.16187*, 2024.
- [47] I. Loshchilov and F. Hutter. Decoupled weight decay regularization. *arXiv preprint arXiv:1711.05101*, 2017.
- [48] H. Lu, C. Zhao, J. Xue, L. Yao, K. Moore, and D. Gong. Adaptive rank, reduced forgetting: Knowledge retention in continual learning vision-language models with dynamic rank-selective lora. *arXiv preprint arXiv:2412.01004*, 2024.
- [49] Z. Luo, Y. Liu, B. Schiele, and Q. Sun. Class-incremental exemplar compression for class-incremental learning. In *Proceedings of the IEEE/CVF Conference on Computer Vision and Pattern Recognition*, pages 11371–11380, 2023.
- [50] S. Maji, E. Rahtu, J. Kannala, M. Blaschko, and A. Vedaldi. Fine-grained visual classification of aircraft. *arXiv preprint arXiv:1306.5151*, 2013.
- [51] M. McCloskey and N. J. Cohen. Catastrophic interference in connectionist networks: The sequential learning problem. In *Psychology of learning and motivation*, volume 24, pages 109–165. Elsevier, 1989.
- [52] M. D. McDonnell, D. Gong, A. Parvaneh, E. Abbasnejad, and A. van den Hengel. Ranpac: Random projections and pre-trained models for continual learning. *Advances in Neural Information Processing Systems*, 36, 2024.
- [53] F. Meng, Z. Wang, and M. Zhang. Pissa: Principal singular values and singular vectors adaptation of large language models. *arXiv preprint arXiv:2404.02948*, 2024.
- [54] K. Meng, D. Bau, A. Andonian, and Y. Belinkov. Locating and editing factual associations in gpt. *Advances in neural information processing systems*, 35:17359–17372, 2022.
- [55] C. V. Nguyen, A. Achille, M. Lam, T. Hassner, V. Mahadevan, and S. Soatto. Toward understanding catastrophic forgetting in continual learning. *arXiv preprint arXiv:1908.01091*, 2019.
- [56] M.-E. Nilsback and A. Zisserman. Automated flower classification over a large number of classes. In *2008 Sixth Indian conference on computer vision, graphics & image processing*, pages 722–729. IEEE, 2008.
- [57] O. M. Parkhi, A. Vedaldi, A. Zisserman, and C. Jawahar. Cats and dogs. In *2012 IEEE conference on computer vision and pattern recognition*, pages 3498–3505. IEEE, 2012.
- [58] F. Qiao and M. Mahdavi. Learn more, but bother less: parameter efficient continual learning. *Advances in Neural Information Processing Systems*, 37:97476–97498, 2024.
- [59] C. Qin and S. Joty. Lfpt5: A unified framework for lifelong few-shot language learning based on prompt tuning of t5. *arXiv preprint arXiv:2110.07298*, 2021.
- [60] A. Radford, J. W. Kim, C. Hallacy, A. Ramesh, G. Goh, S. Agarwal, G. Sastry, A. Askell, P. Mishkin, J. Clark, et al. Learning transferable visual models from natural language supervision. In *International conference on machine learning*, pages 8748–8763. PMLR, 2021.

- [61] C. Raffel, N. Shazeer, A. Roberts, K. Lee, S. Narang, M. Matena, Y. Zhou, W. Li, and P. J. Liu. Exploring the limits of transfer learning with a unified text-to-text transformer. *Journal of machine learning research*, 21(140):1–67, 2020.
- [62] A. Razdaibiedina, Y. Mao, R. Hou, M. Khabsa, M. Lewis, and A. Almahairi. Progressive prompts: Continual learning for language models. *arXiv preprint arXiv:2301.12314*, 2023.
- [63] S.-A. Rebuffi, A. Kolesnikov, G. Sperl, and C. H. Lampert. icarl: Incremental classifier and representation learning. In *Proceedings of the IEEE conference on Computer Vision and Pattern Recognition*, pages 2001–2010, 2017.
- [64] A. A. Rusu, N. C. Rabinowitz, G. Desjardins, H. Soyer, J. Kirkpatrick, K. Kavukcuoglu, R. Pascanu, and R. Hadsell. Progressive neural networks. *arXiv preprint arXiv:1606.04671*, 2016.
- [65] N. Shazeer, A. Mirhoseini, K. Maziarz, A. Davis, Q. Le, G. Hinton, and J. Dean. Outrageously large neural networks: The sparsely-gated mixture-of-experts layer. *arXiv preprint arXiv:1701.06538*, 2017.
- [66] J. S. Smith, L. Karlinsky, V. Gutta, P. Cascante-Bonilla, D. Kim, A. Arbelle, R. Panda, R. Feris, and Z. Kira. Coda-prompt: Continual decomposed attention-based prompting for rehearsal-free continual learning. In *Proceedings of the IEEE/CVF Conference on Computer Vision and Pattern Recognition*, pages 11909–11919, 2023.
- [67] L. Tang, Z. Tian, K. Li, C. He, H. Zhou, H. Zhao, X. Li, and J. Jia. Mind the interference: Retaining pre-trained knowledge in parameter efficient continual learning of vision-language models. In *European Conference on Computer Vision*, pages 346–365. Springer, 2025.
- [68] A. Wang, A. Singh, J. Michael, F. Hill, O. Levy, and S. R. Bowman. Glue: A multi-task benchmark and analysis platform for natural language understanding. *arXiv preprint arXiv:1804.07461*, 2018.
- [69] A. Wang, Y. Pruksachatkun, N. Nangia, A. Singh, J. Michael, F. Hill, O. Levy, and S. Bowman. Superglue: A stickier benchmark for general-purpose language understanding systems. *Advances in neural information processing systems*, 32, 2019.
- [70] F.-Y. Wang, D.-W. Zhou, L. Liu, H.-J. Ye, Y. Bian, D.-C. Zhan, and P. Zhao. Beef: Bi-compatible class-incremental learning via energy-based expansion and fusion. In *The Eleventh International Conference on Learning Representations*, 2022.
- [71] F.-Y. Wang, D.-W. Zhou, H.-J. Ye, and D.-C. Zhan. Foster: Feature boosting and compression for class-incremental learning. In *European conference on computer vision*, pages 398–414. Springer, 2022.
- [72] H. Wang, H. Lu, L. Yao, and D. Gong. Self-expansion of pre-trained models with mixture of adapters for continual learning. *arXiv preprint arXiv:2403.18886*, 2024.
- [73] L. Wang, X. Zhang, H. Su, and J. Zhu. A comprehensive survey of continual learning: Theory, method and application. *IEEE Transactions on Pattern Analysis and Machine Intelligence*, 2024.
- [74] X. Wang, T. Chen, Q. Ge, H. Xia, R. Bao, R. Zheng, Q. Zhang, T. Gui, and X. Huang. Orthogonal subspace learning for language model continual learning. *arXiv preprint arXiv:2310.14152*, 2023.
- [75] Y. Wang, Z. Huang, and X. Hong. S-prompts learning with pre-trained transformers: An occam’s razor for domain incremental learning. *Advances in Neural Information Processing Systems*, 35:5682–5695, 2022.
- [76] Z. Wang, Z. Zhang, S. Ebrahimi, R. Sun, H. Zhang, C.-Y. Lee, X. Ren, G. Su, V. Perot, J. Dy, et al. Dualprompt: Complementary prompting for rehearsal-free continual learning. In *European Conference on Computer Vision*, pages 631–648. Springer, 2022.

- [77] Z. Wang, Z. Zhang, C.-Y. Lee, H. Zhang, R. Sun, X. Ren, G. Su, V. Perot, J. Dy, and T. Pfister. Learning to prompt for continual learning. In *Proceedings of the IEEE/CVF Conference on Computer Vision and Pattern Recognition*, pages 139–149, 2022.
- [78] M. Wortsman, G. Ilharco, J. W. Kim, M. Li, S. Kornblith, R. Roelofs, R. G. Lopes, H. Hajishirzi, A. Farhadi, H. Namkoong, et al. Robust fine-tuning of zero-shot models. In *Proceedings of the IEEE/CVF Conference on Computer Vision and Pattern Recognition*, pages 7959–7971, 2022.
- [79] T. Wu, J. Wang, Z. Zhao, and N. Wong. Mixture-of-subspaces in low-rank adaptation. *arXiv preprint arXiv:2406.11909*, 2024.
- [80] J. Xiao, J. Hays, K. A. Ehinger, A. Oliva, and A. Torralba. Sun database: Large-scale scene recognition from abbey to zoo. In *2010 IEEE computer society conference on computer vision and pattern recognition*, pages 3485–3492. IEEE, 2010.
- [81] Y. Xu, Y. Chen, J. Nie, Y. Wang, H. Zhuang, and M. Okumura. Advancing cross-domain discriminability in continual learning of vision-language models. *arXiv preprint arXiv:2406.18868*, 2024.
- [82] Q. Yan, D. Gong, Y. Liu, A. van den Hengel, and J. Q. Shi. Learning bayesian sparse networks with full experience replay for continual learning. In *Proceedings of the IEEE/CVF Conference on Computer Vision and Pattern Recognition*, pages 109–118, 2022.
- [83] S. Yan, J. Xie, and X. He. Der: Dynamically expandable representation for class incremental learning. In *Proceedings of the IEEE/CVF Conference on Computer Vision and Pattern Recognition*, pages 3014–3023, 2021.
- [84] S. Yang, M. A. Ali, C.-L. Wang, L. Hu, and D. Wang. Moral: Moe augmented lora for llms’ lifelong learning. *arXiv preprint arXiv:2402.11260*, 2024.
- [85] J. Yu, Y. Zhuge, L. Zhang, P. Hu, D. Wang, H. Lu, and Y. He. Boosting continual learning of vision-language models via mixture-of-experts adapters. In *Proceedings of the IEEE/CVF Conference on Computer Vision and Pattern Recognition*, pages 23219–23230, 2024.
- [86] F. Zenke, B. Poole, and S. Ganguli. Continual learning through synaptic intelligence. In *International conference on machine learning*, pages 3987–3995. PMLR, 2017.
- [87] J. Zhang, Y. Zhao, D. Chen, X. Tian, H. Zheng, and W. Zhu. Milora: Efficient mixture of low-rank adaptation for large language models fine-tuning. *arXiv preprint arXiv:2410.18035*, 2024.
- [88] Q. Zhang, M. Chen, A. Bukharin, N. Karampatziakis, P. He, Y. Cheng, W. Chen, and T. Zhao. Adalora: Adaptive budget allocation for parameter-efficient fine-tuning. *arXiv preprint arXiv:2303.10512*, 2023.
- [89] W. Zhang, P. Janson, R. Aljundi, and M. Elhoseiny. Overcoming generic knowledge loss with selective parameter update. In *Proceedings of the IEEE/CVF Conference on Computer Vision and Pattern Recognition*, pages 24046–24056, 2024.
- [90] X. Zhang, J. Zhao, and Y. LeCun. Character-level convolutional networks for text classification. *Advances in neural information processing systems*, 28, 2015.
- [91] Y. Zheng, R. Zhang, J. Zhang, Y. Ye, Z. Luo, Z. Feng, and Y. Ma. Llamafactory: Unified efficient fine-tuning of 100+ language models. In *Proceedings of the 62nd Annual Meeting of the Association for Computational Linguistics (Volume 3: System Demonstrations)*, Bangkok, Thailand, 2024. Association for Computational Linguistics. URL <http://arxiv.org/abs/2403.13372>.
- [92] Z. Zheng, M. Ma, K. Wang, Z. Qin, X. Yue, and Y. You. Preventing zero-shot transfer degradation in continual learning of vision-language models. *arXiv preprint arXiv:2303.06628*, 2023.
- [93] D.-W. Zhou, Q.-W. Wang, H.-J. Ye, and D.-C. Zhan. A model or 603 exemplars: Towards memory-efficient class-incremental learning. *arXiv preprint arXiv:2205.13218*, 2022.

- [94] D.-W. Zhou, H.-L. Sun, H.-J. Ye, and D.-C. Zhan. Expandable subspace ensemble for pre-trained model-based class-incremental learning. In *Proceedings of the IEEE/CVF Conference on Computer Vision and Pattern Recognition*, pages 23554–23564, 2024.

A Additional Details of MoRA

We provide more details of developing the proposed MoRA in this section.

A.1 Model Weights and Updates as Linear Associative Memory Model

Weight matrix as linear associative memory. Large pre-trained models (PTMs) have been shown to inhabit a low “intrinsic-dimension” manifold compared to their full parameter count [1, 41]. Any weight matrix of a pre-trained model $\mathbf{W}_0 \in \mathbb{R}^{d_{\text{out}} \times d_{\text{in}}}$ can be treated as a linear associative memory model with a key-value structure [5, 6, 37, 54]. Concretely, for any matrix $\mathbf{W} \in \mathbb{R}^{d_{\text{out}} \times d_{\text{in}}}$ and input $\mathbf{x} \in \mathbb{R}^{d_{\text{in}}}$, the product $\mathbf{W}\mathbf{x}$ implements a content-addressable memory read over m stored key-value pairs $\{(\mathbf{K}_i, \mathbf{V}_i)\}_{i=1}^m$, where m denotes the number of key-value memories of a specific weight matrix. Here, $\mathbf{K} = [\mathbf{K}_1^\top \ \cdots \ \mathbf{K}_m^\top]^\top \in \mathbb{R}^{m \times d_{\text{in}}}$ and $\mathbf{V} = [\mathbf{V}_1 \ \cdots \ \mathbf{V}_m] \in \mathbb{R}^{d_{\text{out}} \times m}$ with $\mathbf{K}_i \in \mathbb{R}^{1 \times d_{\text{in}}}$ is the i -th row of \mathbf{K} and $\mathbf{V}_i \in \mathbb{R}^{d_{\text{out}} \times 1}$ is the i -th column of \mathbf{V} . Given any input \mathbf{x} , the output $\mathbf{y} \in \mathbb{R}^{d_{\text{out}}}$ is computed as

$$\mathbf{y} = \mathbf{W}\mathbf{x} \approx \sum_{i=1}^m \mathbf{V}_i(\mathbf{K}_i\mathbf{x}). \quad (8)$$

In this formulation, the forward pass through the weight matrix with the input decomposes into two steps: (1) computing response scores or assignment weights via the key vectors \mathbf{K}_i , and (2) aggregating the corresponding value vectors \mathbf{V}_i according to those weights.

Low-rank update as modifications to the linear associative memory. Building on the associative-memory view of weights, we can likewise interpret weight updates during training as key-value insertions into the existing memory. During training, for an arbitrary update $\Delta\mathbf{W}$ on a given \mathbf{W}_0 as the starting point, the weight update process can be represent as

$$\mathbf{W}_{\text{new}} = \mathbf{W}_0 + \Delta\mathbf{W}, \quad (9)$$

where \mathbf{W}_0 can be the pre-trained model weights. We can also formulate the weight updates $\Delta\mathbf{W}$ with the key-value memory model $\{\Delta\mathbf{K}, \Delta\mathbf{V}\}$ as an update to the original memory model. With the operation on an input \mathbf{x} via

$$\Delta\mathbf{W}\mathbf{x} = \Delta\mathbf{V}\Delta\mathbf{K}\mathbf{x}, \quad (10)$$

the updates on weights can be seen as a retrievable key-value system for the updating of $\mathbf{W}\mathbf{x}$.

Low-Rank Adaptation (LoRA) [32] performs parameter-efficient fine-tuning by adding a rank- r update $\Delta\mathbf{W} = \mathbf{B}\mathbf{A}$ to the pre-trained weight matrix \mathbf{W}_0 , where $\mathbf{B} \in \mathbb{R}^{d_{\text{out}} \times r}$ and $\mathbf{A} \in \mathbb{R}^{r \times d_{\text{in}}}$. With the model update based on LoRA, given an input \mathbf{x} , the computation of updated weight becomes

$$\mathbf{y}_{\text{new}} = \mathbf{W}_{\text{new}}\mathbf{x} = \mathbf{W}_0\mathbf{x} + \Delta\mathbf{W}\mathbf{x} = \mathbf{W}_0\mathbf{x} + \mathbf{B}\mathbf{A}\mathbf{x}. \quad (11)$$

Decomposing the low-rank matrices into a collection of its r rank-1 components gives

$$\Delta\mathbf{W}\mathbf{x} = \mathbf{B}\mathbf{A}\mathbf{x} = \sum_{i=1}^r \mathbf{B}_i(\mathbf{A}_i\mathbf{x}), \quad (12)$$

with $\mathbf{A} = [\mathbf{A}_1^\top \ \cdots \ \mathbf{A}_r^\top]^\top \in \mathbb{R}^{r \times d_{\text{in}}}$ where \mathbf{A}_i is the i -th row of \mathbf{A} , and $\mathbf{B} = [\mathbf{B}_1 \ \cdots \ \mathbf{B}_r] \in \mathbb{R}^{d_{\text{out}} \times r}$ where \mathbf{B}_i is the i -th column of \mathbf{B} .

Considering the connection between the formulation of LoRA Eq. (1) and associative-memory view of weight update Eq. (10), we can naturally interpret LoRA as maintaining a small key-value store in a low-rank subspace, where the rows of \mathbf{A} serve as *keys* and the columns of \mathbf{B} serve as their corresponding *values*. After training the LoRA module on a base weight matrix \mathbf{W}_0 , the modified forward pass in Eq. (11) with Eq. (12) can be seen as: first, the original pre-trained computation $\mathbf{W}_0\mathbf{x}$ (Eq. (8)) is performed; then, each learned key \mathbf{A}_i measures its relevance to the input \mathbf{x} via the product $\mathbf{A}_i\mathbf{x}$, and each learned value \mathbf{B}_i is scaled by this relevance score and aggregated, in a same way as shown in Eq. (8). In this way, LoRA effectively inserts or updates a small set of key-value memories that augment the pre-trained model’s capabilities.

A.2 Sparse Mixture-of-Rank Adaptation

In the key-value associative memory view of LoRA (Eq. (11) and Eq. (12)), a standard LoRA or its variants [53, 87] apply a dense, fixed update: every rank’s subspace contributes for any kinds of

input \mathbf{x} . Even in MoE-LoRA, where each LoRA module is treated as a separate expert, all key-value pairs within a LoRA module are used densely as a whole, either fully activated or not activated at all. This leads to redundancy across experts and overlooked the strong potential of the key vectors \mathbf{A} on expressing its relevance to the input.

Rather than activating all key-value memories of each LoRA for all kinds of inputs, where many of which may encode patterns irrelevant to the current input, we introduce a gated, sparse mixture-of-ranks update that selectively activates only the most relevant key-value pairs for each input. Concretely, we associate each rank-1 key-value pair with a scalar weight $w_i \in \mathbb{R}$, so that for an input token $\mathbf{x} \in \mathbb{R}^{d_{\text{in}}}$ from task t , with r_t total ranks, the update becomes:

$$\Delta \mathbf{W}^t = \sum_{i=1}^{r_t} w_i \mathbf{B}_i \mathbf{A}_i, \text{ and } \Delta \mathbf{W}^t \mathbf{x} = \sum_{i=1}^{r_t} w_i \mathbf{B}_i \mathbf{A}_i \mathbf{x}, \quad (4)$$

where w_i modulates whether and how strongly the corresponding rank contributes to the final updated weight matrix.

As discussed in Sec. 3.4, rather than obtaining mixture weights w_i 's through learning an additional router [72, 85], considering that \mathbf{A}_i 's in \mathbf{A} works as keys in the memory model that reflect the significance on the correlation between input and the learned knowledge in each rank, we leverage the key vectors \mathbf{A}_i themselves to infer each rank's relevance. Specifically, w_i 's are obtained through sparsity-inducing scaling with top-k masking and rank pruning of each rank's activation $\mathbf{A}_i \mathbf{x}$, *i.e.*, $[w_i] = \text{SparseOperator}([\mathbf{A}_i \mathbf{x}])$, where $\text{SparseOperator}()$ denotes the sparse-inducing operations.

Our fine-grained mixture framework offers two key advantages: (1) It reduces redundancy and enables shared-knowledge reuse: ranks that capture common, cross-task features (such as generic semantics) can be reactivated across multiple tasks, preventing those patterns from being relearned redundantly or interfered; (2) It minimizes routing ambiguity and prevents forgetting: each rank can specialize on more nuanced patterns, yielding an optimized, rank-wise mixture that integrates new knowledge without disrupting existing representations or hindering future updates.

B Additional Details and Results of Experiments

Table 6: Details of the 15 datasets used in our continual-learning experiments using LLM. NLI denotes natural language inference, and QA denotes question-answering tasks. The first five tasks comprise the standard CL benchmark; the remaining ten tasks are used for the extended long-sequence evaluations.

Dataset name	Category	Task	Domain	Metric
1. Yelp	CL Benchmark	sentiment analysis	Yelp reviews	accuracy
2. Amazon	CL Benchmark	sentiment analysis	Amazon reviews	accuracy
3. DBpedia	CL Benchmark	topic classification	Wikipedia	accuracy
4. Yahoo	CL Benchmark	topic classification	Yahoo Q&A	accuracy
5. AG News	CL Benchmark	topic classification	news	accuracy
6. MNLI	GLUE	NLI	various	accuracy
7. QQP	GLUE	paragraph detection	Quora	accuracy
8. RTE	GLUE	NLI	news, Wikipedia	accuracy
9. SST-2	GLUE	sentiment analysis	movie reviews	accuracy
10. WiC	SuperGLUE	word sense disambiguation	lexical databases	accuracy
11. CB	SuperGLUE	NLI	various	accuracy
12. COPA	SuperGLUE	QA	blogs, encyclopedia	accuracy
13. BoolQA	SuperGLUE	boolean QA	Wikipedia	accuracy
14. MultiRC	SuperGLUE	QA	various	accuracy
15. IMDB	SuperGLUE	sentiment analysis	movie reviews	accuracy

B.1 Detailed Experiment Settings

CL on CLIP. We follow the experimental setups in [81, 85, 92] and use the CLIP model with a ViT-B/16 backbone [60] for all experiments. By default, MoRA is applied to every pre-trained weight

Table 7: Instructions for different tasks.

Task	Prompts
NLI	What is the logical relationship between the "sentence 1" and the "sentence 2"? Choose one from the option.
QQP	Whether the "first sentence" and the "second sentence" have the same meaning? Choose one from the option.
SC	What is the sentiment of the following paragraph? Choose one from the option.
TC	What is the topic of the following paragraph? Choose one from the option.
BoolQA	According to the following passage, is the question true or false? Choose one from the option.
MultiRC	According to the following passage and question, is the candidate answer true or false? Choose one from the option.
WiC	Given a word and two sentences, whether the word is used with the same sense in both sentence? Choose one from the option.

Table 8: The six task-sequence orders used in our continual learning experiments. Sequences 1–3 follow the standard CL benchmarks employed in prior work. Sequences 4–6 extend to longer 15-task streams, as introduced in [62].

Order	Task Sequence
1	dbpedia → amazon → yahoo → ag
2	dbpedia → amazon → ag → yahoo
3	yahoo → amazon → ag → dbpedia
4	mnli → cb → wic → copa → qqp → boolqa → rte → imdb → yelp → amazon → sst-2 → dbpedia → ag → multirc → yahoo
5	multirc → boolqa → wic → mnli → cb → copa → qqp → rte → imdb → sst-2 → dbpedia → ag → yelp → amazon → yahoo
6	yelp → amazon → mnli → cb → copa → qqp → rte → imdb → sst-2 → dbpedia → ag → yahoo → multirc → boolqa → wic

matrix in both the vision and text encoders, with an initial rank of 16 per update. Each task is trained for 500 iterations using AdamW [47] with learning rate of $5e - 4$. During continual learning, we freeze the ranks learned from previous tasks and initialize new $r = 16$ ranks for each incoming task. The rank activation budget is set to 16 throughout all tasks. We set the temperature $\tau_{\text{MoRA}} = 0.1$ and the threshold $\delta = 0.2$.

CL on LLMs. We follow the protocol of previous work in continually fine-tuning a T5-large model on a suite of text-classification tasks. We train on five standard benchmarks—AG News, Amazon Reviews, Yelp Reviews, DBpedia, and Yahoo Answers—using three distinct task orderings drawn from [58, 59, 62, 74]. To probe longer sequences, we extend this to a 15-dataset stream (Table 6), incorporating tasks from the original CL benchmark [90], GLUE [68], SuperGLUE [69], and the IMDB movie reviews corpus. Natural language prompts for each task are presented in Table 7, with NLI tasks (MNLI, RTE, CB), sentiment classification (Amazon, Yelp, SST-2, IMDB), and topic classification (AG News, DBpedia, Yahoo).

We evaluate three distinct task sequences for both the standard CL and 15-task benchmarks (Table 8). After completing the final task in each stream, we report the average accuracy across all tasks. All experiments use one epoch per task with DeepSpeed, a fixed learning rate of $1e - 3$, batch size 64, and dropout of 0.1. MoRA is applied to both the query and key projection matrices within attention layers, initializing $r = 8$ new ranks for each incoming task similarly as in [58, 74]. We maintain a constant activation budget of 4 ranks throughout continual learning, set the temperature $\tau_{\text{MoRA}} = 0.1$, and the threshold $\delta = 0.2$.

Generalization and forgetting on unseen tasks. To assess effects on pre-trained general knowledge, we fine-tune Llama3.1-8B [28] on the CodeAlpaca code-generation dataset [9] using llama-Factory [91] and evaluate using lm-eval-harness [26] on zero-shot in-domain performance on HumanEval [12], as well as out-of-domain accuracy on a broad selection of MMLU [31] subjects—Formal Logic, Philosophy, World Religions, Economics, Public Relations, STEM, Physics, and Machine Learning.

In this experiment, MoRA is applied to all linear weight matrices of the pre-trained model. We fine-tune on CodeAlpaca with a batch size of 32 over 3 epochs and a cosine learning-rate schedule starting at $5e - 4$. We train with $r = 16$ ranks and enforce a constant activation budget of 4 ranks. The self-routed gating uses a temperature $\tau_{\text{MoRA}} = 0.5$ and a threshold $\delta = 0.2$. We observe that, due to variations in hidden representations across architectures, the optimal temperature setting can differ across each pre-trained models.

Reproducibility Statement. Our source code will be publicly released upon paper acceptance. Results are averaged over three independent runs to ensure robustness. Experiments with the CLIP model were carried out on an NVIDIA GeForce RTX 3090 GPU, while experiments with LLMs utilized 4 NVIDIA H100 GPUs.

Table 9: Average accuracy on T5-large continual-learning benchmarks after the final task, evaluated over extended 15-task sequences. Results for prior methods are taken from [58].

Method	Large Number of Tasks			Avg.
	Order-4	Order-5	Order-6	
MTL	76.5			
SeqFT	7.4	7.4	7.5	7.4
SeqLoRA	2.3	0.6	1.9	1.6
IncLoRA	63.3	58.5	61.7	61.2
Replay	55	54.6	53.1	54.2
EWC	45.3	44.5	45.6	45.1
LwF	50.1	43.1	47.4	46.9
L2P	57.5	53.8	56.9	56.1
LFPT5	69.8	67.2	69.2	68.7
O-LoRA	70.5	65.5	70.5	68.8
LB-CL	68.4	67.3	71.8	69.2
MoRA	68.91	68.32	71.95	69.72

B.2 Continual Learning of LLM on Long Task Sequences

In Sec. 4.2 Table 3, we evaluate MoRA on standard CL benchmarks [62]. In Table 9, we extend the evaluation to challenged long task sequences using 15 datasets with 3 different orderings as in [58, 74]. Consistent with the findings in Table 3, MoRA outperforms previous methods in terms of averaged performance across three task orders, and largely close the gap to multi-task learning. Two key design choices drive this robust performance in the long-sequence regime. First, by decomposing each LoRA update into fine-grained rank-1 components and enforcing a small, fixed activation budget, MoRA encourages each rank to specialize on a narrow subspace of the data manifold. At inference time, only the most relevant subspaces are activated for a given input, which preserves earlier task representations and prevents catastrophic interference. Second, our self-routed gating mechanism enables each rank to assess its own relevance on a per-token basis, yielding stable mixture patterns as the expert pool grows. Coupling with our proposed rank pruning, these mechanisms ensure that MoRA continually incorporates new knowledge only when needed while robustly maintaining prior capabilities.

B.3 Computation Cost

Table 10 summarizes the per-task trainable parameters of various continual-learning methods. Standard LoRA [32], CoDyRA [48], and O-LoRA [74] each introduce $r(d_{\text{in}} + d_{\text{out}})$ new parameters per weight matrix. Mixture-of-Experts variants such as MoE-LoRA and MoE-Adapter [85] additionally train a router module to control the usage of each LoRA experts, inducing d_{in} additional parameters for each experts. LB-CL [58] introduce r additional parameters, mimic the singular values of SVD.

By contrast, MoRA requires only $r d_{\text{in}} + k d_{\text{out}}$ activated trainable parameters per task, where $k \leq r$ is the activation budget, and the trainable parameter is at most the same as a standard LoRA. Despite the small number of parameter activated and trained, MoRA achieves superior continual learning performance, and reaches comparable performance in general fine-tuning with only one-third of the activated parameters of a standard LoRA.

Table 10: Comparisons of trainable parameters for each pre-trained weight matrix during continual learning of each task. MoE-LoRA and MoE-Adapter trains additional router module with LoRA experts. In MoRA, k denotes the rank activation budget (with $k \leq r$).

Method	Trainable parameters per task
LoRA [32]	$r(d_{in} + d_{out})$
MoE-LoRA (1 expert/task)	$r(d_{in} + d_{out}) + d_{in}$
MoE-Adapter (2 experts/task) [85]	$2(r(d_{in} + d_{out}) + d_{in})$
CoDyRA [48]	$r(d_{in} + d_{out})$
O-LoRA [74]	$r(d_{in} + d_{out})$
LB-CL [58]	$r(d_{in} + d_{out}) + r$
MoRA	$rd_{in} + kd_{out}$

B.4 Extended Visualizations of Rank Activations

In Sec.4.4 (Fig.3), we illustrated rank activations during the learning of Task 1 and Task 2. Here, we extend these visualizations to additional tasks and scenarios in Fig.5 and Fig.6.

MoRA retains task-specific semantics without forgetting. Fig. 5 shows the activation maps for the same Task 1 image after training on Task 1 (a), Task 2 (b), and the last Task 10 (c). Patches corresponding to the airplane object are outlined in orange. In all three snapshots, Rank at index 0 remains consistently and exclusively activated for those airplane patches, demonstrating that MoRA has effectively memorized the airplane-specific knowledge into Rank 0. Even after 10 subsequent tasks, this pattern remains unchanged, indicating that later updates do not overwrite or interfere with the learned airplane representations. In other words, MoRA effectively memorizes and preserves task-relevant semantics, thereby mitigating catastrophic forgetting.

MoRA encodes generic semantics that are reused across tasks. Fig. 6 examines an input image from Task 9 before and after learning Task 9. Panel (a) shows the activation map of data from Task 1 after learning Task 1: Rank 11 (outlined in blue) already responds strongly to sky-background patches, demonstrating that MoRA has stored a generic “blue sky” concept in this rank. In panel (b), when we infer on the Task 9 image before training on Task 9, Rank 11 is again activated for the sky regions, confirming that MoRA reuses this shared knowledge for unseen data. Finally, panel (c) shows the activation map after learning Task 9: Rank 11 remains dedicated to the sky background, while newly initialized ranks specialize in the “car” object semantics. This persistent reuse of Rank 11 across tasks illustrates MoRA’s ability to capture and retain common features as reusable memory slots, reducing redundancy and facilitating knowledge reuse.

B.5 Statistical Analyses of Contributing Rank Activations

Fig. 7 and Fig. 8 plot the cumulative sum of averaged rank activations after training on all tasks, sorted in descending order, for several representative layers and locations within pre-trained models. The red dashed line marks the point at which 99% of the total activation mass is reached, allowing us to quantify how many ranks are truly contributing to the model’s adaptation. Two key observations emerge:

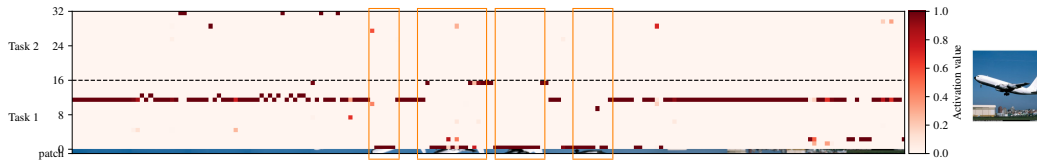
1. Sparse Mixture: only a small subset of ranks is needed. Across all layers and positions, we find that fewer than 10% of the total ranks suffice to capture 99% of the activations. This highlights the extreme sparsity of MoRA’s self-activated mixture: most ranks remain dormant for any given input, while a compact set of highly relevant ranks drives the adaptation.

2. Adaptive Activation: The number of ranks required varies by layers and modules. The number of ranks needed to capture 99% of the cumulative activation mass varies across both layer depth and module type. For example, in Fig. 7, the MLP’s output projection (c-proj) in Layer 1 of the vision encoder requires 16 ranks, whereas the same module in Layer 1 of the text encoder needs only 3 ranks.

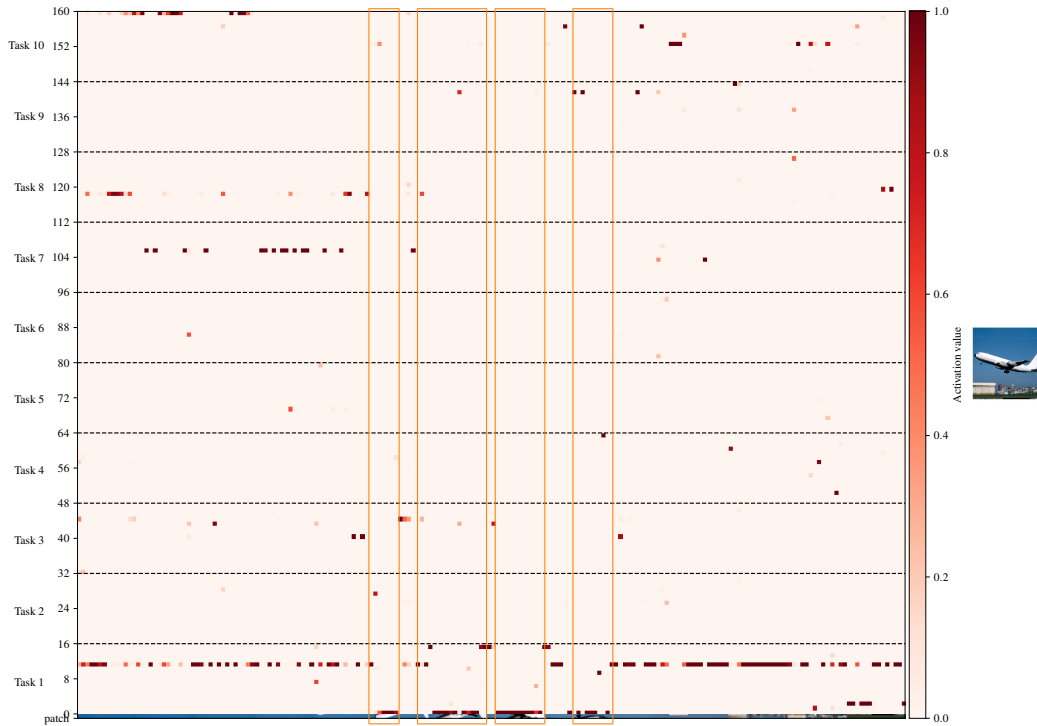
To provide a broader view, Fig. 9 shows the required rank counts for every module in the pre-trained model. We observe that most attention modules requires around 6–12 ranks, while the second MLP



(a) Rank Activations of MoRA on data from Task 1 after learning Task 1.



(b) Rank Activations of MoRA on data from Task 1 after learning Task 2.



(c) Rank Activations of MoRA on data from Task 1 after learning Task 10.

Figure 5: Extended view of Fig. 3 illustrating **forgetting mitigation**. Regions corresponding to object semantics are highlighted with orange bounding boxes. Zoom in for details.

projection generally demands more ranks in early layers, peaking in the first few blocks, and then steadily declines in deeper layers.

Coupling the rank activation budget with rank pruning, MoRA adapts the number of ranks needed to activate at each layer and module. This adaptive sparsity maximizes the efficient use of newly acquired knowledge during continual learning.

Broader Impacts

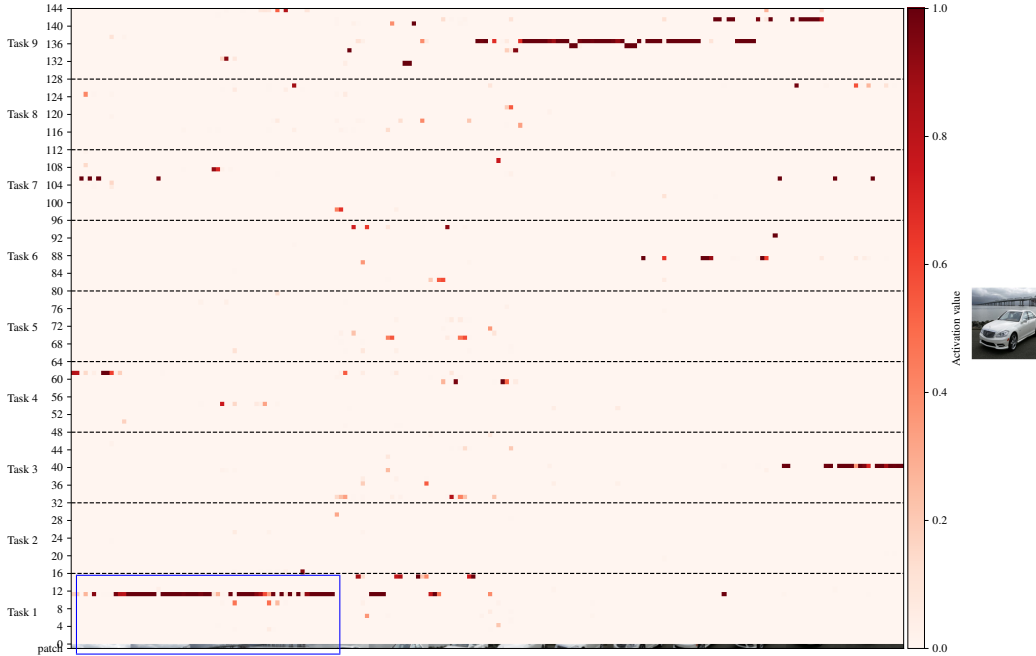
MoRA’s self-activated, sparse mixture-of-ranks method makes continual adaptation of large vision–language and language models far more efficient and reliable. By updating only the most relevant low-rank subspaces, it reduce compute and memory requirements, enabling on-device personalization in domains like education, healthcare, and finance. This democratizes access to powerful, continually evolved models for smaller teams and resource-constrained settings, driving innovation and improving quality of life. Preserving pre-trained knowledge also ensures stability in safety-critical systems, such as medical diagnostics and autonomous vehicles, where forgetting of pre-trained capabilities can be dangerous.



(a) Rank Activations of MoRA on data from Task 1 after learning Task 1.



(b) Rank Activations of MoRA on data from Task 9 after learning Task 1.



(c) Rank Activations of MoRA on data from Task 9 after learning Task 9.

Figure 6: Extended view of Fig. 3 illustrating **knowledge reuse**. Regions corresponding to generic input tokens (*e.g.* blue sky) are highlighted with blue bounding boxes. Zoom in for details.

The focus of this paper is fundamental research, and is broadly applicable to model fine-tuning techniques. Thus, it is possible that MoRA’s lightweight updates could be misused to insert stealthy backdoors or reinforce hidden biases that are hard to detect. Because it leaves most pre-trained parameters untouched, existing biases may persist or become entrenched. To mitigate these risks, we recommend strict audit logging of rank-level updates, anomaly detection on sparse changes, robust access controls, and routine bias and fairness assessments alongside any deployment.

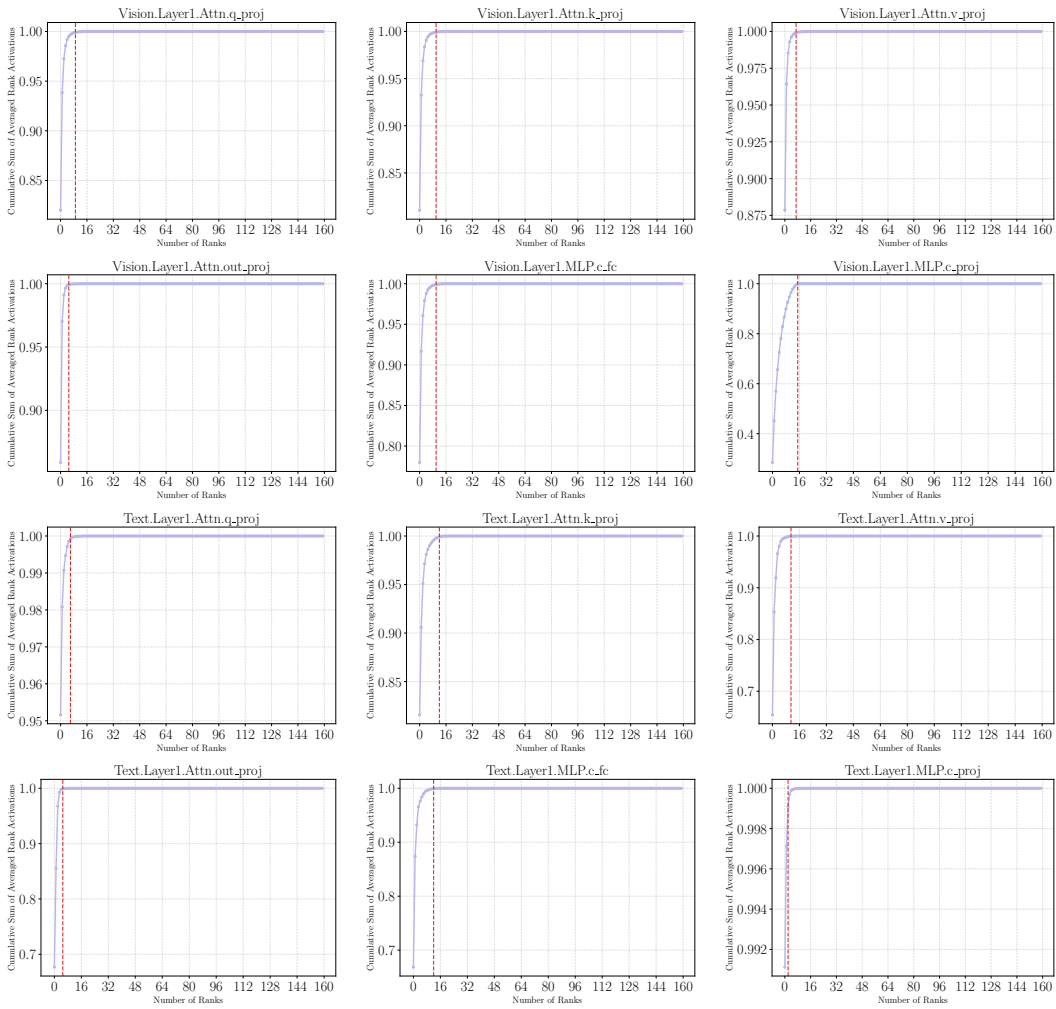


Figure 7: Statistical analyses on the number of ranks required to capture 99% of cumulative sum (indicated in red dashed line) of all rank activations. Activations were gathered from the model after training on all tasks, and results are shown for a representative selection of layers and positions within the pre-trained model.

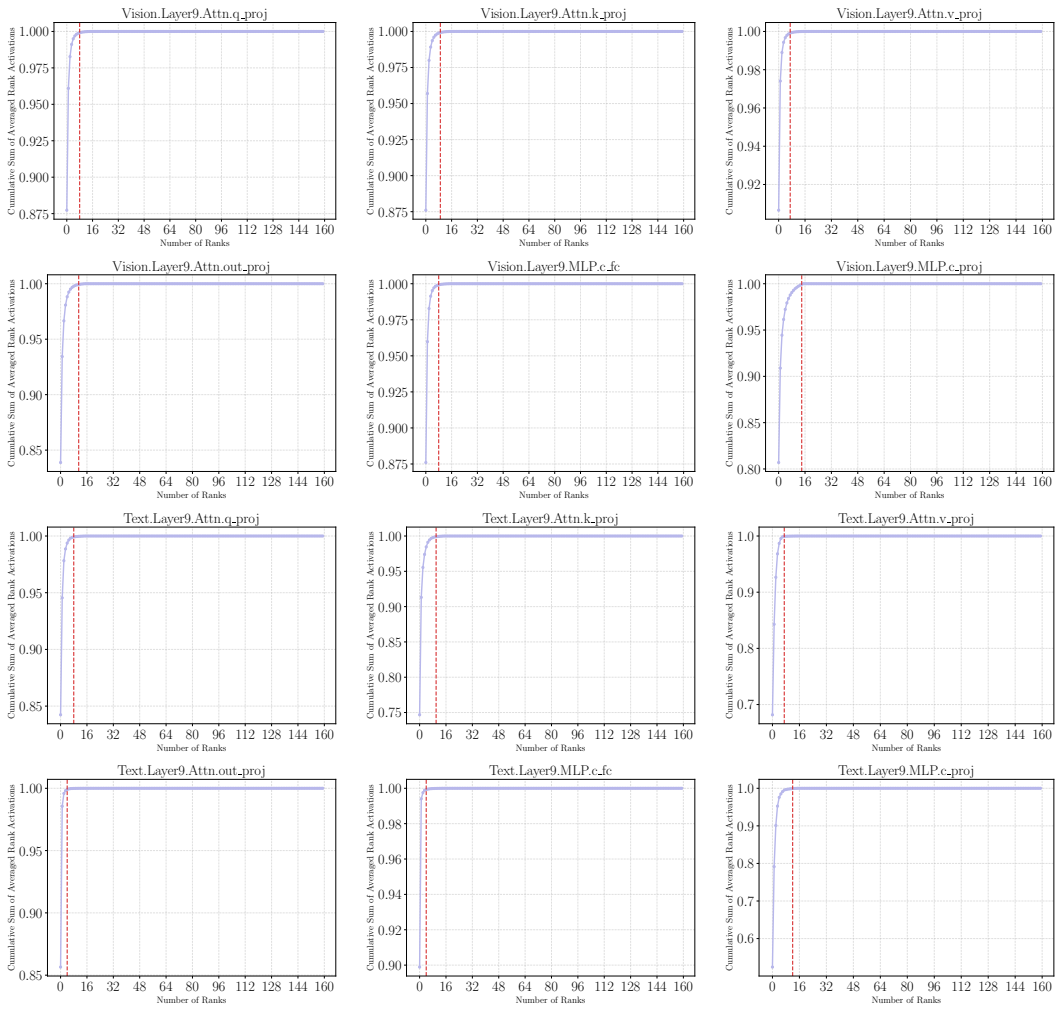


Figure 8: Statistical analyses on the number of ranks required to capture 99% of cumulative sum (indicated in red dashed line) of all rank activations. Activations were gathered from the model after training on all tasks, and results are shown for a representative selection of layers and positions within the pre-trained model.

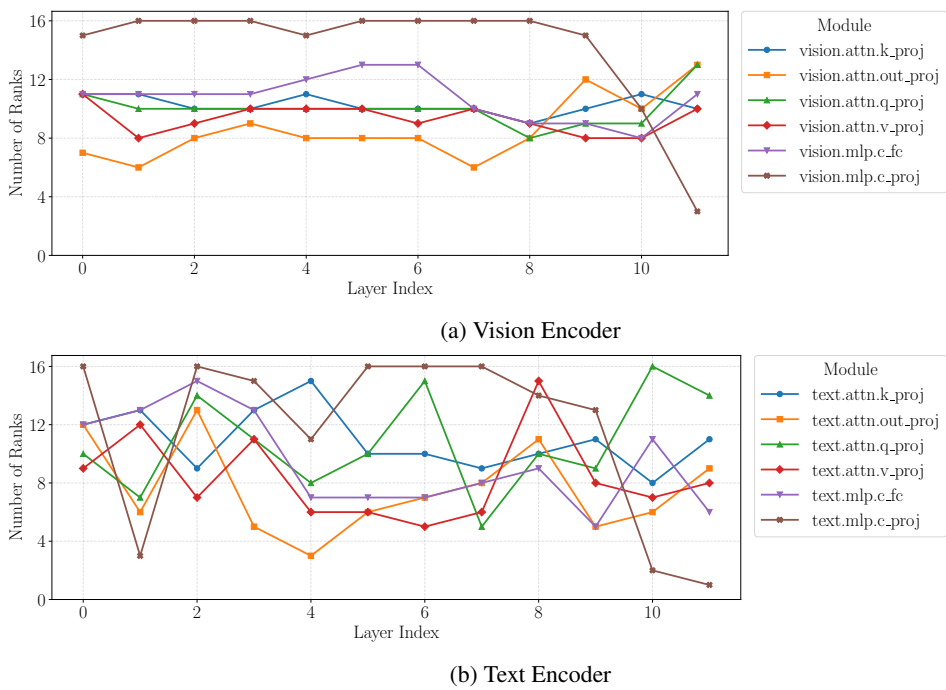


Figure 9: Required ranks to capture 99 % of cumulative activations, shown across different pre-trained model layers and projection locations.